Level Structure of the Odd-A Isotopes of Samarium*

ROBERT A. KENEFICK† AND RAYMOND K. SHELINE
The Florida State University, Tallahassee, Florida
(Received 3 May 1965)

The levels of Sm^{145}, Sm^{149}, Sm^{151}, Sm^{153}, and Sm^{155} have been studied with 0.1% resolution by the (d,p) reaction at 12-MeV incident energy. Levels in Sm^{147} have been observed by (p,p') reactions at 12 MeV. A large number of previously unknown levels have been observed at excitation energies up to 4 MeV. Previously known levels from decay spectroscopy have, in general, been verified. It is suggested that spherical and deformed nuclear shapes are in evidence close to the ground state in Sm^{151}. This conclusion is based partly on these data, on the spectroscopic structure of the neighboring even-even nuclei Sm^{150} and Sm^{152}, and on the observed two-neutron separation energies (S_{2n}) of odd-A and even-A Sm isotopes in this transition region. A fragmentation of the (d,p) intensities among the increasing number of states is observed as one proceeds from Sm^{145} (single closed shell plus one neutron) to Sm^{155} (strongly deformed), as expected from the Nilsson model. Some of the levels below 2 MeV in Sm^{145} are discussed in terms of shell-model configurations. Levels in Sm^{147} are compared with the $(f_{7/2})^3$ coupling scheme and with the excited-core model. Using particularly the relative intensities of members of the rotational bands, which strongly characterize the assignments, but also the observed energies for the levels and systematics of other deformed odd-A nuclei, the following Nilsson orbitals and some of their associated rotational states have been assigned in Sm^{153} and Sm^{155}: $\frac{3}{2}-$ (521), $\frac{5}{2}-$ (523), $\frac{1}{2}-$ (521) and $\frac{5}{2}+$ (642). The (d,p) spectra indicate that the ground state of Sm^{153} is the $\frac{3}{2}+$ (651) configuration and not the $\frac{3}{2}-$ (521) as assumed previously. The ground state for Sm^{155} is assigned as the $\frac{3}{2}-$ (521) orbital. The previously unobserved $(11/2)-$ (505) orbital, whose depopulation is hypothesized to cause the sudden onset of deformation at $N=90$, has been tentatively assigned at 65 keV in Sm^{153}. The ground-state Q values observed in the experiments are: $Sm^{144}(d,p)Sm^{145}$, $Q=+4.533\pm0.012$ MeV; $Sm^{148}(d,p)Sm^{149}$, $Q=+3.648\pm0.012$ MeV; $Sm^{150}(d,p)Sm^{151}$, $Q=+3.369\pm0.016$ MeV; $Sm^{152}(d,p)Sm^{153}$, $Q=+3.645\pm0.012$ MeV; $Sm^{154}(d,p)Sm^{155}$, $Q=+3.584\pm0.012$ MeV.

I. INTRODUCTION

THE levels of heavy deformed odd-A nuclei in the rare-earth and actinide regions have been the subject of recent intensive investigation. It has been shown recently [1,2] that the (d,p) reaction is particularly useful in studying these levels because it relates in a direct way to the deformed-core-plus-odd-nucleon model[3] of Nilsson. The (d,p) reaction on spherical nuclei can be treated as a special case where the deformation parameter $\delta=0$. The usefulness of the (d,p) reaction has been considerably extended by the development of the distorted-wave Born approximation (DWBA) theory,[4] which allows l values to be determined and fairly reliable reduced widths to be extracted. DWBA analysis has also developed a quantitative description of the (p,p') reaction.[5]

This paper represents an interpretation of (d,p) and (p,p') data for the odd-A isotopes of samarium. The stable isotopes of this element extend from $N=82$ (closed shell) to $N=92$ (highly deformed). Therefore, the changes in level structure associated with the transition from a spherical to a deformed shape may be studied in a rather systematic manner. When combined with previous decay studies, these data provide a great deal of additional information on these nuclei.

II. EXPERIMENTAL METHOD

The experimental method has been described in detail in previous publications[6,7]; only the main points will be given here. A beam of deuterons or protons from the Florida State University Tandem Van de Graaff was analyzed by a 90° magnet, deflected by another magnet and focused by a quadrupole lens system to strike thin targets of isotopically enriched samarium oxide. The target material was obtained from the Separated Isotopes Division of Oak Ridge National Laboratories. The enrichments for targets used in these experiments are given in Table I. The oxides were evaporated by an electron-gun technique[8] onto thin (10–30 $\mu g/cm^2$) car-

TABLE I. Enriched samarium oxides for target fabrication.

Enriched isotope \ A	Percentages of samarium isotopes						
	144	147	148	149	150	152	154
Sm^{144}	71.50	9.23	4.14	3.25	1.41	3.91	6.62
Sm^{147}	0.08	97.80	0.91	0.51	0.17	0.34	0.21
Sm^{148}	0.36	0.81	96.26	1.41	0.34	0.55	0.28
Sm^{150}	0.10	1.00	1.40	8.40	81.0	6.50	1.60
Sm^{152}	0.03	0.20	0.20	0.27	0.30	97.20	1.80
Sm^{154}	0.02	0.12	0.09	0.12	0.08	0.50	99.07

* Supported by the U. S. Atomic Energy Commission under Contract AT-(40-1)-2434. The Florida State University Tandem Van de Graaff was supported by the U. S. Air Force Office of Scientific Research under Contract AFOSR-62-423 and by the Nuclear Program of the State of Florida.

† Present address: Department of Physics, University of Michigan, Ann Arbor, Michigan.

[1] M. N. Vergnes and R. K. Sheline, Phys. Rev. **132**, 1736 (1963).

[2] R. K. Sheline, W. N. Shelton, H. T. Motz, and R. E. Carter, Phys. Rev. **136**, B351 (1964).

[3] S. G. Nilsson, Kgl. Danske Videnskab. Selskab, Mat. Fys. Medd. **29**, No. 16 (1955).

[4] R. H. Bassel, R. M. Drisko, and G. R. Satchler, Atomic Energy Commission Report ORNL-3240 (unpublished).

[5] H. O. Funsten, N. R. Roberson, and E. Rost, Phys. Rev. **134**, B117 (1964).

[6] R. A. Kenefick and R. K. Sheline, Phys. Rev. **133**, B25 (1964).

[7] W. N. Shelton and R. K. Sheline, Phys. Rev. **133**, B624 (1964).

[8] M. C. Olesen and B. Elbek, Nucl. Phys. **15**, 26 (1960).

bon films. Targets prepared for these experiments ranged in thickness from 50 to 300 μg/cm^2. The beam spot was defined to $\frac{1}{4}\times 3$ mm.

The target was located at the object point of a 60 cm pole-face radius Browne-Buechner[9] type magnetic analyzer.

Eastman NTA 50 μ track plates were used as detectors. In the (d,p) experiments, thin aluminum foils were secured on the emulsion surfaces to stop deuterons and alpha particles. The plates were scanned in $\frac{1}{2}\times 8$ mm strips with dark-field illuminated microscopes equipped with calibrated stages.

The spectrograph solid angle was typically 2.2×10^{-4} sr during most of the experiments described here. Typical best energy resolution achieved in these experiments is approximately 0.1%.

In these experiments the incident energy, Q values, and level energies were determined either by the position of elastic scattering groups or by the position of the following groups:

$$C^{12}(d,p)C^{13}, \quad (Q_0=2722.3\pm 0.3 \text{ keV})$$
$$C^{13}(d,p)C^{14}, \quad (Q_0=5931.4\pm 0.5 \text{ keV})$$
$$O^{16}(d,p)O^{17}, \quad (Q_0=1917.4\pm 0.8 \text{ keV}).$$

These reference peaks were combined with the previously determined calibration curve in a consistent manner.

III. SUMMARY OF PREVIOUS WORK

The decay of Eu^{145} has been studied by Anton'eva *et al.*[10] They deduced levels at $894(\frac{3}{2}^-)$, $1004(\frac{1}{2}^-)$, $1663(\frac{5}{2}^-)$, 1880, 2001, and 2424 keV. All observed transitions were fitted into the decay scheme except a line corresponding to $E_\gamma=191$ keV. The Sm^{145} ground state was taken as $(\frac{7}{2}^-)$ from shell-model considerations. A more recent study[11] showed additional levels at 1550 and 1870 keV.

The conversion lines from the decay of Eu^{147} have been measured with a magnetic spectrometer by Anton'eva *et al.*,[10] and by Schwerdtfeger *et al.*[12] These studies have established levels at $121(\frac{5}{2}^-)$, $198(\frac{3}{2}^-)$, $800(\frac{5}{2},\frac{3}{2}^-)$, $1079(\frac{3}{2}, \frac{5}{2}, \frac{7}{2}, \text{or } \frac{9}{2}^-)$ and 1420 (?) keV. In another study[13] of the Eu^{147} decay the same levels were deduced. Considerable evidence for a level at 900 keV has been put forth.[14] Nathan and Popov[15] have observed Coulomb excitation of a state at 730 keV. The ground states of Sm^{147} and Sm^{149} have been measured as $\frac{7}{2}$ from optical hyperfine structure,[16] paramagnetic resonance,[17] and atomic-beam magnetic resonance experiments.[18] In a recent review[19] of Sm^{147}, additional levels were assigned at 1060, 1320, 1448, and 1545 keV.

Levels in Sm^{149} have been observed by Harmatz *et al.*[20] From the conversion electron- and gamma-ray spectrum of the decay of Eu^{149}, levels in Sm^{149} at 22.5, 277.2, 350.2, 528.6, and 558.3 keV were proposed. The Eu^{149} decay was also studied by Dzhelepov *et al.*,[21] using a β spectrometer and gamma-gamma coincidence methods. Their results were in agreement with Harmatz *et al.* Levels at 285 keV $(\frac{5}{2}, \frac{7}{2}^-)$, 582 keV $(\frac{9}{2}^-)$, 833 keV, and 850 keV $(\frac{3}{2}, \frac{5}{2}, \frac{7}{2}^-)$ were proposed by Schmid and Burson[22] from a study of the Pm^{149} decay. In addition to these studies, Nathan and Popov[15] have reported Coulomb excitation of a level at $\sim$650 keV in Sm^{149}.

Sm^{151} has been studied through the decay[23–26] of Pm^{151} and also through the reaction $Sm^{150}(n,\gamma)Sm^{151}$ with a bent crystal γ-ray spectrometer.[27] This has resulted in the establishment of sixteen levels up to 821-keV excitation. In addition, β-γ and γ-γ angular correlation data for a few of these states are available[28] although their interpretation is not definite.

Two gamma rays of 125 keV and 180 keV have been observed[29] in the decay of Pm^{153} to Sm^{153}. In addition, gamma rays with the following energies have been seen[30] with a crystal spectrometer following the reaction $Sm^{152}(n,\gamma)Sm^{153}$: 35.8, 90.88, 119.78, 127.30, 166.65, 175.37, and 182.90 keV. A level scheme was deduced in Ref. 30 from the above gamma energies, but this scheme is not in good agreement with the data to be presented here.

In the case of Sm^{155}, no previous information has been published on the level scheme.

---

[9] C. P. Browne and W. W. Buechner, Rev. Sci. Instr. **27**, 899 (1956).
[10] N. M. Anton'eva, A. A. Bashvilov, B. S. Dzhelepov, K. G. Kaun, A. F. A. Meyer, and V. B. Smirnov, Zh. Eksperim. i Teor. Fiz. **40**, 23 (1961) [English transl.: Soviet Phys.—JETP **13**, 15 (1961)].
[11] Yu. A. Aleksandrov and M. K. Nikitin, Izvest. Akad. Nauk SSSR, Ser. Fiz., **25**, 1176 (1961).
[12] C. F. Schwerdtfeger, E. G. Funk, and J. W. Mihelich, Phys. Rev. **125**, 1641 (1962).
[13] S. Jha, H. G. Devare, and G. C. Pramila, Nuovo Cimento **25**, 28 (1962).
[14] B. S. Dzhelepov, K. Gromov, I. Vizi, Yu. Yazvitsky, and Zh. Zhelev, Nucl. Phys., **30**, 120 (1962).
[15] O. Nathan and V. Popov, Nucl. Phys. **21**, 631 (1961).
[16] K. Murakawa and J. S. Ross, Phys. Rev. **82**, 967 (1951).
[17] G. S. Bogle and H. E. D. Scovil, Proc. Phys. Soc. (London) **A65**, 366 (1952).
[18] I. J. Spalding and K. F. Smith, Proc. Phys. Soc. (London) **79**, 787 (1962).
[19] J. F. McNulty, E. G. Funk, and J. W. Mihelich, Nucl. Phys. **55**, 657 (1964).
[20] B. Harmatz, T. H. Handley, and J. W. Mihelich, Phys. Rev. **123**, 1758 (1961).
[21] B. S. Dzhelepov, K. Gromov, A. Kudryavtseva, Fu-Ch'ing Wang, I. Vizi, Yu. Yazvitsky, and Zh. Zelev, Nucl. Phys. **30**, 110 (1962).
[22] L. C. Schmid and S. C. Burson, Phys. Rev. **120**, 158 (1960).
[23] B. Harmatz, T. H. Handley, and J. W. Mihelich, Phys. Rev. **128**, 1186 (1962).
[24] D. G. Burke, M. E. Law, and M. W. Johns, Can. J. Phys. **41**, 57 (1963).
[25] U. Bertelsen, G. T. Ewan, and H. L. Nielsen, Nucl. Phys. **50**, 657 (1964).
[26] L. Funke, H. Graber, K. H. Kaun, H. Sodan, and L. Werner (to be published).
[27] J. S. Geiger and R. L. Graham, quoted as a private communication in Ref. 24.
[28] R. Chery, Nucl. Phys. **32**, 319 (1962).
[29] K. Kotajima, Nucl. Phys. **39**, 89 (1962).
[30] Otto W. B. Schult, Z. Naturforsch. **16a**, 927 (1961).

TABLE II. Results for $Sm^{144}(d,p)Sm^{145}$. The numbers for assigned levels correspond to the peak numbers in Fig. 1.

Level No.	Q (keV)	Excitation energy (keV)	Relative intensity (60°)	Other Sm isotope[a] A	% of peak
0	4533(12)	0	100.0		
	4254(15)		0.3	148	100
	4185(15)		0.7	148	100
	4018(12)		3.0	148	100
	3943(15)		0.6	148	100
	3818(15)		1.1	148	100
	3770(14)		0.15	148	100
	3703(12)		1.0	148	100
1	3638(8)	895(4)	92.0	149	~3
	3591(10)		2.6	155	75
2[b]	3529(10)	1004?(6)	1.5	148	~95
	3462(10)		2.5	155	~80
3	3425(8)	1108(4)	8.3	148	~10
	3394(8)		3.0	148	100
	3365(10)		1.0	150	~70
	3302(10)		1.0	150	~60
	3277(8)		2.2	148	100
	3245(9)		1.5	150	~75
	3195(9)		2.0	148	~60
	3163(9)		1.4	148	~60
4	3106(6)	1427(6)	19.0	150	~8
	3087(9)		1.5	155	100
	3058(9)		1.4	151	~65
	2992(9)		0.6	148	100
	2947(9)		1.8	150	40
5	2922(6)	1611(9)	44.0		
6	2868(5)	1665(8)	...		
	2818(8)		1.0	148	~70
	2764(5)		5.0	155	~55
7	2749(5)	1784(8)	8.0	148	~10
8	2723(5)	1810(8)	4.6		
9	2679(6)	1854(9)	8.5	155	65
10	2650(5)	1883(8)	17.0	155	~15
11	2554(5)	1979(8)	40.0		
12	2531(5)	2002(8)	41.0		
	2487(8)		3.0	150	~65
	2454(12)		1.0	148	100
13	2421(10)	2112(14)	1.5	151	70
14	2395(5)	2138(9)	24.0	148	~6
15	2369(5)	2164(9)	23.0	148	~10
16	2334(12)	2199(16)	1.0	150	~90
	2303(12)		2.0	148	~60
	2263(12)		1.0	148	~80
17	2236(5)	2297(9)	21.0		
	2204(10)		1.0	150	~100
18	2184(4)	2349(10)	8.0		
	2158(12)		0.5	148	~55
19	2143(4)	2390(10)	4.6	148	~35
20	2104(4)	2429(10)	17.0		
	2074(12)		...	148	~55
21	2045(10)	2488(15)	1.5	148	~40
22	2021(10)	2512(15)	1.0	150	~80
	2002(12)		1.0	155	100
23	1970(5)	2563(11)	5.0	150	~50
	1931(10)		...	150	100
24	1902(9)	2629(15)	4.0	150	~80
25	1872(11)	2661(17)	2.0	148	~40
26	1843(3)	2690(12)	17.0		
27	1809(10)	2724(16)	2.0	150	~50
28	1783(12)	2750(18)	1.5	150	~25
29	1736(5)	2797(12)	}		
30	1709(7)	2824(14)	}13.0	148	~15
31	1691(10)	2842(19)	}		
	1657(6)		2.0	155	~100
32	1607(3)	2926(13)	4.5		
33	1573(6)	2960(16)	2.0		
34	1515(3)	3018(13)	20.0		
	1494(5)		...	155	~100
35	1441(3)	3092(13)	31.0		
36	1401(3)	3132(13)	36.0		
37	1350(5)	3183(15)	...		
38	1287(10)	3246(20)	5.0		
39	1258(10)	3275(20)	3.0		
40	1231(3)	3302(13)	18.0		
41	1198(7)	3335(17)	5.0		
42	1167(4)	3366(14)	20.0		
43	1136(4)	3397(14)	}		
44	1100(7)	3433(17)	}48.0		
45	1087(10)	3446(20)	}		
46	1053(10)	3480(20)	9.0		
47	1025(10)	3506(20)	3.0		
48	999(10)	3534(20)	2.0		
49	975(4)	3558(14)	18.0		
50	937(4)	3596(14)	...		
51	900(11)	3633(21)	...		
52	878(11)	3655(21)	...		
53	854(4)	3679(14)	20.0		
54	807(4)	3726(14)	8.0		
55	750(5)	3783(15)	17.0		
56	700(5)	3833(15)	14.0		
57	677(11)	3856(21)	3.0		
58	651(5)	3882(15)	17.0		
59	617(10)	3916(20)	11.0		
60	523(10)	4010(20)	2.0		
61	506(5)	4027(15)	24.0		

[a] When there is no Sm^{145} contribution to the peak, the dominant isotope and its percentage contribution are listed; when there is a Sm^{145} contribution, the most important contributing isotope is indicated, but the percentage shown is the contribution of all other (i.e., $A \neq 145$) Sm isotopes to the peak.

[b] Although decay work places a level at this energy the observed (d,p) intensity is accounted for by $Sm^{147}(d,p)Sm^{148}$.

IV. RESULTS AND Q VALUES

Sm^{145}

Proton spectra for the reaction $Sm^{144}(d,p)Sm^{145}$ were observed at 45° and 60°. The 60° spectrum is shown in Fig. 1. Note that groups 0 (ground state) and 1 are reduced by $\frac{1}{4}$, and groups 12 and 36 by $\frac{1}{2}$ in vertical scale. The solid angle subtended by the analyzer was 2.2×10^{-4} sr for these spectra. Unlabeled groups were assigned to light impurities by their kinematic shift.

Owing to the relatively low enrichment in Sm^{144}, a large number of levels from other isotopes of samarium have been observed. These have, for the most part, been accounted for, since the (d,p) spectra of these other isotopes have been determined.[6] The peak at $Q=+3529$ keV, which is a known Q value for $Sm^{147}(d,p)Sm^{148}$, is only slightly stronger than would be expected from the intensities of other groups due to the reaction $Sm^{147}(d,p)$-Sm^{148}. If the increase is assumed due to a state at 1004-keV excitation in Sm^{145}, this state is very weakly excited by (d,p) reaction. For this reason the state is considered tentative. Q values, excitation energies, relative intensities, and isotopic assignments are given in Table II. The ground-state Q value for $Sm^{144}(d,p)Sm^{145}$ was determined to be $+4533\pm12$ keV.

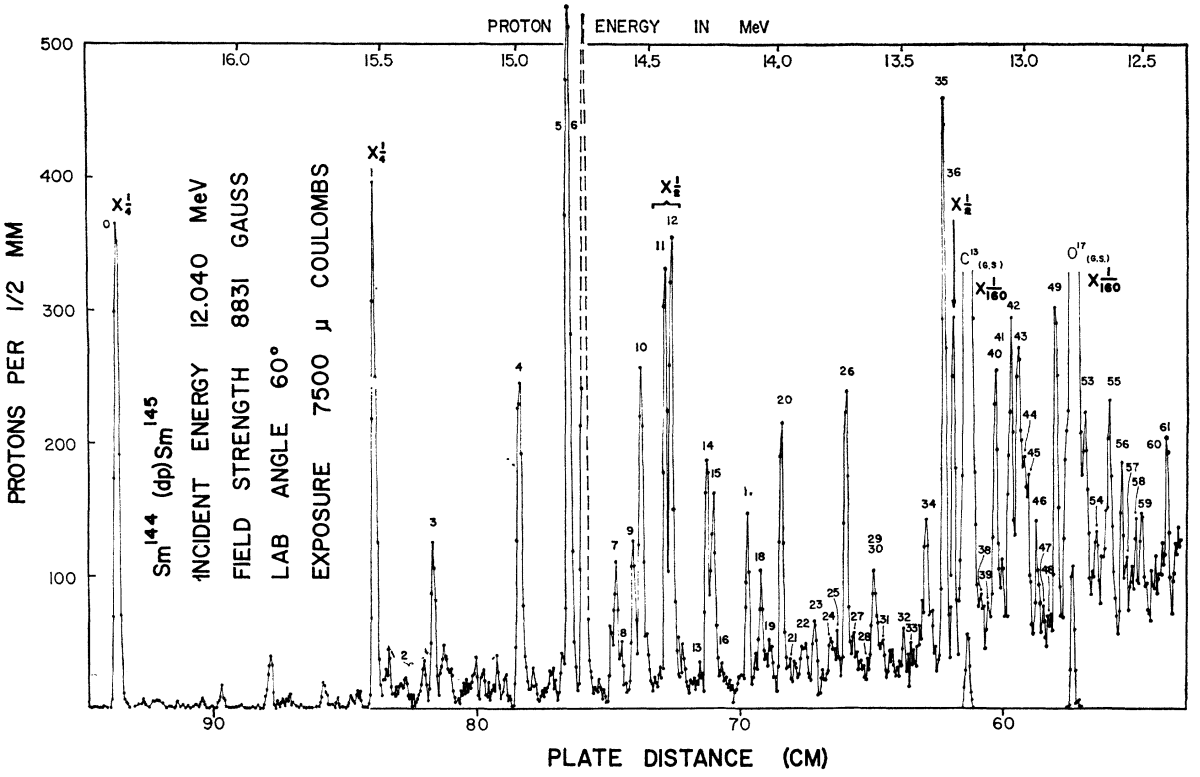

FIG. 1. The $Sm^{144}(d,p)Sm^{145}$ proton spectrum at 60°. Only the groups assigned as levels in Sm^{145} are numbered.

Sm^{147}

The reaction $Sm^{147}(p,p')Sm^{147}$ was studied at 122½° and 133° with an incident proton energy of 12 MeV. The main exposures were 4000 and 7500 μC, respectively, for these angles. Beam spot size during these experiments was ½×3 mm and the solid angle subtended by the spectrograph was 3.5×10^{-4} sr. The 133° spectrum is shown in Fig. 2. Groups from Sm^{147} are numbered sequentially, beginning with zero for the elastic group, which appears in reduced scale at the left. Peaks from the elastic scattering on target impurities are labeled. Level No. 4 is obscured by the Cl^{35} peak in the displayed spectrum (133°), as is level 21 (obscured by

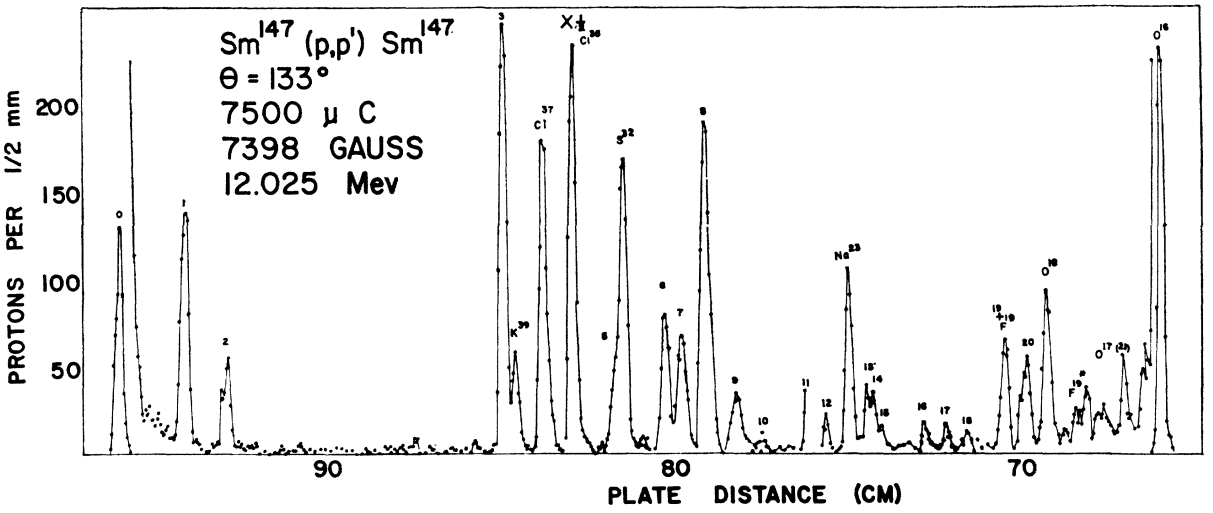

FIG. 2. The proton spectrum at 133° for $Sm^{147}(p,p')Sm^{147}$. Groups from Sm^{147} levels are numbered and light impurity peaks are labeled.

the F^{19} ground state). Level No. 6 appears on the front edge of the S^{32} elastic peak. Only the front edge of level No. 13 is seen at 133° because it, unfortunately, is located at a joint in the track plate array. All levels except level No. 22 are observed, or inferred by intensity changes, at both reaction angles. Two very weak groups are observed at both angles. These levels (levels 5 and 7) check well in energy at the two angles of observation. However, because of their rather low intensity they are considered as tentative. A level scheme for Sm^{147} based on these spectra is shown in Fig. 3.

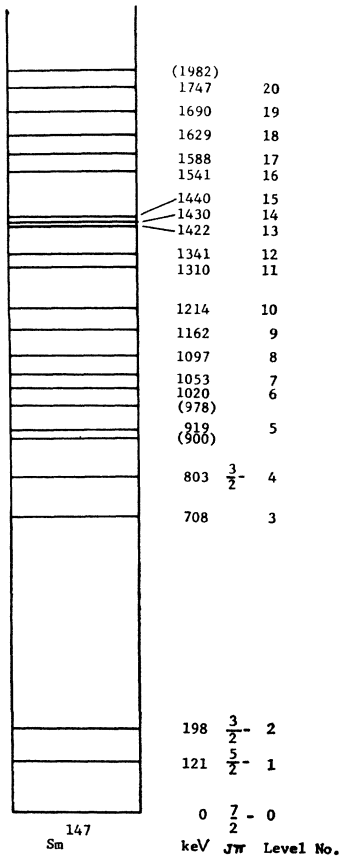

FIG. 3. A level scheme for Sm^{147} from these data. Spins and parities shown to the right are from other experiments. The level numbers correspond to those in Fig. 2.

Sm^{149}

Several different targets of Sm^{148} enriched oxide were used to study the levels in Sm^{149}. The spectra were taken at 45°, 65°, and 133°. One of the 65° spectra is shown in Fig. 4. As in the $Sm^{144}(d,p)Sm^{145}$ spectra, the $\frac{7}{2}$— ground state is strongly excited. This ground-state group displays a definite broadening at its base on the low-energy side. This was observed at all angles and could be accounted for by a peak with intensity $\sim 1/100$ of the ground state located 20–25 keV from it. On some occasions such a broadening has been observed to be due to target thickness or slit scattering. However, if such were the case, all peaks in the spectrum should show the same characteristic shape. This is not the case in these spectra and a level is therefore tentatively placed at ~ 22 keV, in agreement with previous work.

The group at 285-keV excitation (levels No. 2 and 3)

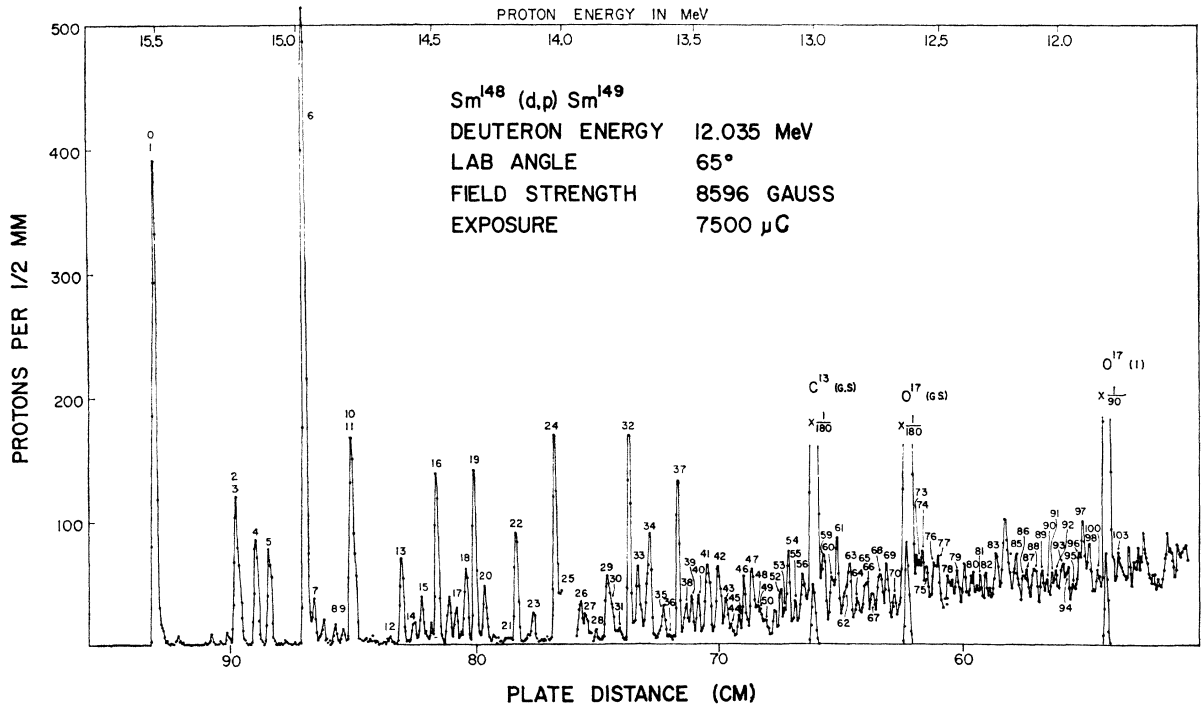

FIG. 4. The $Sm^{148}(d,p)Sm^{149}$ proton spectrum at 65°. Only the groups from Sm^{149} are numbered.

TABLE III. Results for $Sm^{148}(d,p)Sm^{149}$. The level numbers correspond to peak numbers in Fig. 4.

Level No.	Q (keV)	Excitation energy (keV)	Relative intensity (65°)	l value
0	3648(12)	0	1.00	3, 4
1	3628(14)	20(8)	0.01	
2	3368(11)	280(2)	0.38	≥3
3	3363(11)	285(2)		
4	3298(11)	350(2)	0.23	0, 1, 2
5	3250(10)	398(3)	0.19	0, 1, 2
6	3113(10)	535(3)	1.31	0, 1, 2
7	3082(10)	566(3)	0.04	
8	3008(10)	640(3)	0.03	3, 4
9	2975(10)	675(3)	0.03	≥3
10	2948(9)	700(4)	0.52	
11	2936(11)	712(6)		
12	2806(11)	842(6)	0.01	≥3
13	2767(8)	881(5)	0.16	≥3
14	2720(10)	928(7)	0.05	
15	2692(8)	956(5)	0.09	3, 4
16	2635(7)	1013(6)	0.31	0, 1, 2
17	2564(9)	1084(8)	0.07	
18	2523(9)	1125(8)	0.15	
19	2490(7)	1158(6)	0.34	
20	2458(9)	1190(8)	0.12	3, 4
21	2368(11)	1280(10)	0.01	3, 4
22	2332(6)	1316(7)	0.16	3, 4
23	2263(9)	1385(10)	0.07	3, 4
24	2183(5)	1465(6)	0.39	
25	2164(8)	1484(9)	...	3, 4
26	2092(5)	1556(6)	0.10	≥3
27	2069(7)	1579(8)	0.08	3, 4
28	2027(8)	1621(9)	0.03	
29	1986(8)	1662(9)	0.24	
30	1970(10)	1678(15)	...	
31	1943(7)	1705(13)	0.03	
32	1896(3)	1752(10)	0.36	
33	1866(3)	1782(10)	0.17	
34	1832(3)	1816(10)	0.28	
35	1767(6)	1881(13)	0.09	0, 1, 2
36	1738(8)	1910(15)	0.02	
37	1705(3)	1943(10)	0.27	
38	1673(5)	1975(12)	0.10	
39	1649(5)	1999(12)	0.10	≥3
40	1624(5)	2024(12)	0.09	
41	1589(3)	2059(10)	0.24	
42	1547(3)	2101(10)	0.23	
43	1511(5)	2137(12)	0.10	
44	1489(8)	2159(15)	0.04	
45	1457(8)	2191(15)	0.06	
46	1438(3)	2210(10)	0.14	
47	1406(3)	2242(10)	0.19	
48	1384(8)	2264(15)	0.09	
49	1368(8)	2280(15)	0.07	
50	1353(8)	2295(15)	0.07	
51	1316(8)	2332(15)	0.06	
52	1290(6)	2358(13)	0.11	
53	1271(8)	2377(15)	0.05	
54	1261(3)	2387(10)	0.19	
55	1230(4)	2418(11)	0.10	
56	1205(4)	2443(11)	0.15	
57	1154(4)	2494(11)	...	
58	1140(4)	2508(11)	...	
59	1114(4)	2534(11)	0.17	
60	1080(4)	2568(11)	0.16	
61	1058(4)	2590(11)	0.26	
62	1026(4)	2622(11)	0.12	
63	1008(4)	2640(11)	0.18	
64	977(4)	2671(11)	0.14	
65	937(4)	2711(11)	0.12	
66	925(8)	2723(15)	0.09	
67	911(5)	2737(12)	0.14	
68	886(5)	2762(12)	0.24	
69	851(5)	2797(12)	0.19	
70	818(5)	2830(12)	0.13	
71	790(5)	2858(12)	...	
72	757(5)	2891(12)	...	
73	725(5)	2923(12)	0.13	
74	699(5)	2949(12)	0.22	
75	680(5)	2968(12)	0.18	
76	653(5)	2995(12)	0.18	
77	633(5)	3015(12)	0.24	
78	575(5)	3072(12)	0.13	
79	554(5)	3094(12)	0.19	
80	488(5)	3160(12)	0.10	
81	454(5)	3194(12)	0.13	
82	430(5)	3218(12)	0.16	
83	391(6)	3257(13)	2.71	
84	345(6)	3303(13)	0.42	
85	324(6)	3324(13)	0.18	
86	271(6)	3377(12)	0.17	
87	255(7)	3393(14)	0.17	
88	229(7)	3419(14)	0.10	
89	212(7)	3436(14)	0.20	
90	187(7)	3461(14)	0.15	
91	170(7)	3478(14)	0.13	
92	115(7)	3533(14)	0.21	
93	103(8)	3545(15)	0.20	
94	73(8)	3575(15)	0.22	
95	53(8)	3595(15)	0.12	
96	25(8)	3623(15)		
97	12(8)	3336(15)		
98	−13(8)	3661(15)		
99	−39(8)	3687(15)		
100	−52(8)	3700(15)		
101	−86(8)	3734(15)		
102	−117(8)	3765(15)		
103	−158(8)	3806(15)		

is one millimeter greater in width at half-maximum than the neighboring peaks. This indicates the presence of two levels of approximately equal intensity separated by ~8 keV. Similarly, the group at 700 keV (levels No. 10 and 11) is 1.5 mm broader than its neighboring groups. This indicates two levels separated by approximately 12 keV. The 712-keV upper member of this doublet appears from the shape of the peak to be approximately one-half as intense as the 700-keV member.

A level at 1484-keV excitation (level No. 22) is not observable in the 65° spectrum because it happened to fall at a joint in the nuclear emulsion surface.

No peaks were found in the spectrum that could be attributed to the other samarium isotopes known to be present (see Table I). Q values, relative intensities, and excitation energies for the peaks from $Sm^{148}(d,p)Sm^{149}$ are given in Table III. The ground-state Q value for the reaction $Sm^{148}(d,p)Sm^{149}$ is determined by these experiments to be 3648 ± 12 keV.

Sm^{151}

Spectra were obtained at 45°, 65°, 90°, and 133° for the reaction $Sm^{150}(d,p)Sm^{151}$. This target had a particularly thick carbon backing and it proved difficult to obtain high-resolution spectra, due primarily to energy spread introduced by the carbon. Light impurities were

TABLE IV. Results for $Sm^{150}(d,p)Sm^{151}$. Level numbers correspond to the peaks numbered in Fig. 5.

Level No.	Q (keV)	Excitation energy (keV)	Relative intensity (45°)	Other Sm isotope[a] A	% of peak
	3645(12)		1.00	150	85
	3579(14)		0.50	155	80
	3465(13)		0.54	153	70
	3384(14)		0.54	153	100
0	3369(16)	0	1.84	150	25
1	3309(10)	60(2)	17.00		
2	3284(12)	83(4)	1.87		
	3246(12)		1.17	153	60
3	3232(12)	137(3)			
4	3203(12)	166(3)	9.10	150	15
5	3159(12)	210(3)	0.45	150	50
	3141(12)		0.29	150	100
	3114(10)		1.04	153	60
	3097(14)		0.15	153	50
6	3062(9)	307(4)	26.4		
7	3018(12)	351(7)	1.21	150	40
	2950(10)		2.11	153	60
8	2921(8)	448(6)	5.14		
9	2900(8)	469(6)	2.91	150	35
	2760(13)		0.73	150	60
	2722(13)		0.71	153	100
10	2700(7)	669(8)	3.88		
11	2665(7)	704(8)	8.56		
12	2655(11)	714(13)			
13	2614(7)	755(8)	1.65		
	2565(11)		0.15	150	70
	2535(11)		0.40	150	50
14	2524(8)	845(12)	2.79		
15	2491(8)	878(12)	1.7		
16	2483(8)	886(12)	1.1		
17	2418(5)	951(10)	12.20		
18	2351(5)	1018(10)	3.39		
	2305(10)		0.50	150	100
19	2290(10)	1079(18)	2.82		
20	2180(6)	1189(14)	2.92		
21	2156(4)	1213(12)	7.88		
22	2105(4)	1264(12)	2.96		
23	2061(4)	1308(12)	3.15		
23′	2024(4)	1345(12)	6.00		
24	1974(4)	1395(12)	3.80		
25	1956(8)	1413(16)	5.77		
26	1925(4)	1444(12)	5.66		
	1742(10)		6.09		
	1677(10)		4.85		
	1664(10)				
	1648(10)				
	1609(10)		2.22		
	1576(10)		0.78		
	1562(10)		4.79		
	1550(10)				
	1536(10)				
	1503(10)				
	1479(10)		5.24		
	1468(10)				
	1430(10)		...		
	1365(10)		1.21		
	1336(10)		2.37		
	1185(10)		4.00		
	1117(10)		2.48		
	1078(10)		3.90		
	1031(10)		2.57		
	1001(10)		2.15		
	972(10)		6.69		
	935(10)		2.00		
	878(10)		8.15		

[a] Same as footnote a for Table II.
[b] Although many of these peaks are from $Sm^{150}(d,p)Sm^{151}$ the high level density, relatively poor enrichment of the target, and uncertain light impurities do not allow their definite assignment from these data.

extracted from the spectra by their kinematic shift in the usual manner. In addition, because of the relatively low enrichment, considerable care had to be taken in locating (d,p) reaction groups from other samarium isotopes. The result of this extraction is given in Table IV for the 45° spectrum (Fig. 5) including all the assigned groups and their relative intensities. The highest energy group not assignable to another samarium isotope is a doublet at $Q=3368-3384$ keV. The 3384-keV member is partly due to a state in Sm^{153}. For all the nuclei included in this study, but especially here in Sm^{151}, the high level density for Q values less than +2 MeV makes elimination of peaks due to other isotopes very difficult, and some erroneous assignments of weak states in this range are to be expected. Further consideration of the levels of Sm^{151} is given in Sec. V.

Sm^{153}

Proton spectra for the reaction $Sm^{152}(d,p)Sm^{153}$ were taken at 12 MeV at 25°, 35°, 45°, 65°, and 133°. The 35° spectrum is shown in Fig. 6. The 65° spectrum showed rather good resolution, approaching 6 to 8 keV. Groups were assigned to impurities in the usual manner. No observed groups were assignable to the small quantities of other samarium isotopes known to be present. Q values for all Sm^{153} groups were in excellent agreement between the various angles. The ground-state Q value for the reaction $Sm^{152}(d,p)Sm^{153}$ is determined as 3645 ±12 keV. Although the ground-state group is not strong it is observed at all angles in good energetic agreement and is considered a quite certain assignment. Table V gives the Q values, excitation energies, and relative intensities at 45°.

Sm^{155}

Several targets enriched in Sm^{154} were utilized in this study, primarily because of breakage due to inferior backings. A large number of spectra was taken (25°, 35°, 45°, 65°, 133°) at incident energies from 10.4 to 12.6 MeV. A typical spectrum is shown in Fig. 7. The 10.5-MeV spectrum at 65° gave the best resolution, which was approximately 9 keV. Only groups assigned to Sm^{155} are numbered. We discuss here only groups about whose existence there might be some question. Groups No. 1, 2, and 3 are extremely weak and appear clearly only at 45° in a spectrum at 10.5 MeV. At other angles they are either obscured or too weak to be seen (however, at 45° group No. 2 is seen in the 12 MeV-spectra). Groups No. 7 and 8 shift greatly in intensity from angle to angle and are assigned mainly on the basis of the 133° spectrum, where they are relatively strong. Groups No. 11 and 12 are weak, but appear at both 65° (10.5 MeV) and 45° (12 MeV); the other spectra are inconclusive. Group No. 12 could, however, be due to Cl^{36} in the 65° spectrum, as could group No. 15 at 65°. Group No. 38 is not assignable to any expected impurity but appears strongly only at 65°. Q values for

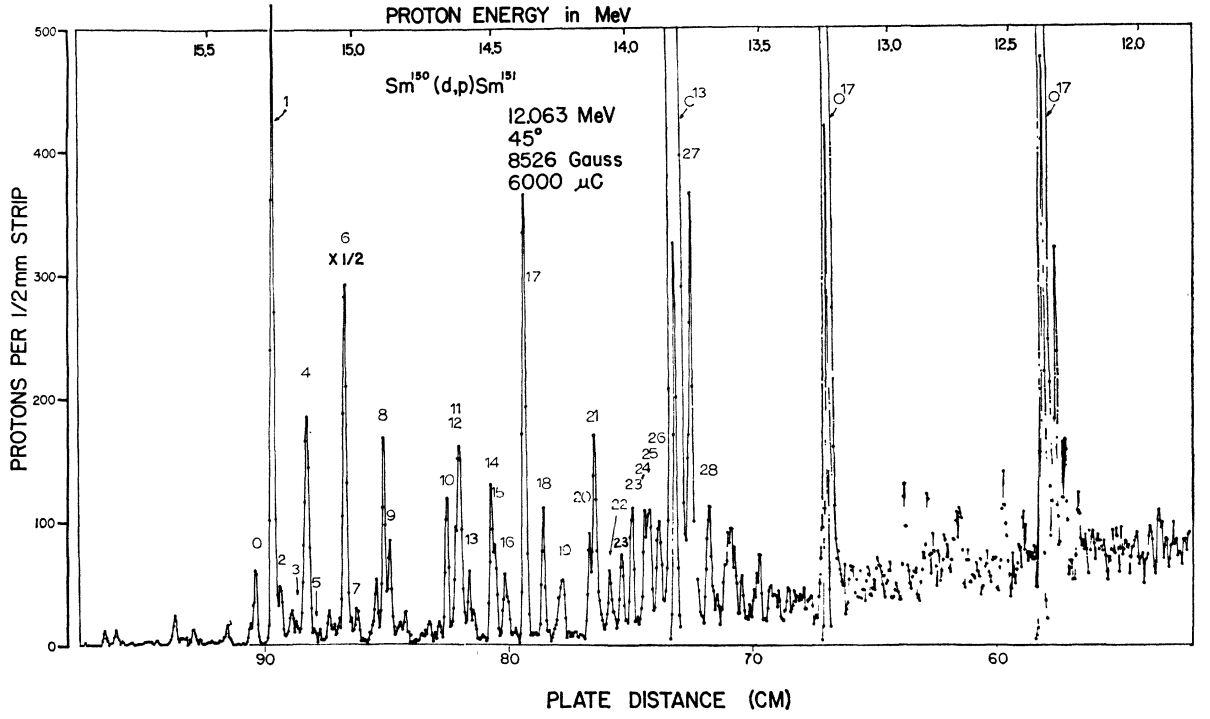

FIG. 5. The $Sm^{150}(d,p)Sm^{151}$ proton spectrum at 45°. Only groups assigned to Sm^{151} are numbered.

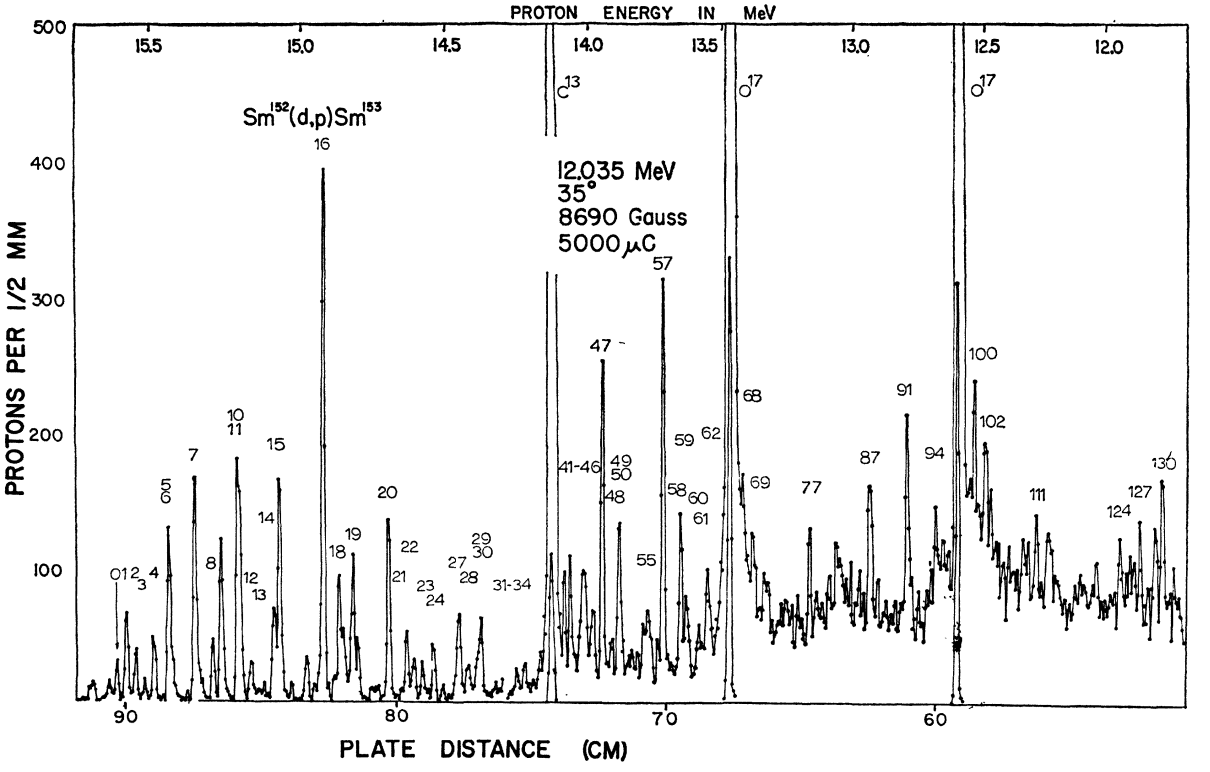

FIG. 6. The $Sm^{152}(d,p)Sm^{153}$ proton spectrum at 35°. Only the groups from Sm^{153} are numbered.

TABLE V. Results for $Sm^{152}(d,p)Sm^{153}$. Numbers for the levels correspond to peak numbers in Fig. 6.

Level No.	Q (keV)	Excitation energy (keV)	Relative intensity (35°)	l value
0	3645(12)	0	1.00	0, 1, 2
1	3610(12)	35(2)	2.50	0, 1, 2
2	3580(12)	65(2)	1.40	≥3
3	3554(14)	91(4)	0.53	0, 1, 2
4	3520(12)	125(2)	1.80	0, 1, 2
5	3469(11)	176(3)	5.80	≥3
6	3463(14)	182(5)		
7	3383(11)	262(3)	6.80	≥3
8	3323(13)	322(5)	1.75	0, 1, 2
9	3275(14)	370(6)	...	
10	3234(10)	411(4)	5.90	
11	3225(13)	420(7)	6.40	
12	3195(10)	450(4)	1.15	0, 1, 2
13	3144(13)	501(7)	0.42	≥3
14	3118(10)	527(4)	3.40	≥3
15	3097(10)	548(4)	7.00	≥3
16	2947(9)	698(5)	13.50	0, 1, 2
17	2906(12)	736(8)	0.69	
18	2891(10)	754(6)	3.90	0, 1, 2
19	2846(9)	799(5)	4.70	≥3
20	2722(8)	923(6)	5.00	≥3
21	2679(11)	966(9)	0.38	
22	2658(8)	987(6)	2.00	
23	2579(8)	1066(6)	0.26	
24	2565(8)	1081(6)	1.75	
25	2531(9)	1114(7)	0.48	
26	2506(9)	1139(7)	0.20	
27	2477(7)	1168(7)	3.40	
28	2441(7)	1204(7)	1.60	
29	2389(12)	1256(12)	...	
30	2416(12)	1229(12)	...	
31	2350(10)	1295(14)	0.39	
32	2335(10)	1310(10)	...	
33	2318(10)	1327(12)	...	
34	2296(10)	1349(12)	0.30	
35	2278(6)	1349(12)	1.30	
36	2250(6)	1396(8)	1.40	
37	2214(8)	1431(10)	0.88	
38	2173(8)	1472(10)	...	
39	2154(10)	1491(12)	...	
40	2139(6)	1506(8)	...	
41	2105(6)	1540(8)	3.90	
42	2081(6)	1564(8)	5.35	
43	2042(5)	1603(9)	8.20	
44	2033(8)	1612(12)		
45	2021(8)	1624(12)		
46	2002(5)	1643(9)	4.50	
47	1966(5)	1679(9)	9.10	
48	1926(5)	1719(9)	2.35	
49	1904(5)	1741(9)	7.17	
50	1894(8)	1751(12)	...	
51	1871(8)	1774(12)	1.80	
52	1853(8)	1792(12)	1.70	
53	1833(8)	1812(12)	1.10	
54	1815(5)	1830(9)	2.70	
55	1807(8)	1838(12)	3.00	
56	1758(7)	1887(11)	1.90	
57	1742(5)	1903(9)	11.20	
58	1710(10)	1935(14)	1.66	
59	1677(5)	1968(12)	5.90	
60	1654(3)	1991(10)	4.50	
61	1616(3)	2029(10)	3.60	
62	1569(3)	2076(10)	3.00	
63	1524(8)	2121(15)	...	
64	1517(8)	2128(15)	...	
65	1501(8)	2144(15)	...	
66	1480(8)	2165(15)	...	
67	1457(8)	2188(15)	...	
68	1443(5)	2202(12)	11.50	
69	1405(6)	2240(16)	7.90	
70	1359(5)	2286(11)	5.25	
71	1343(7)	2302(14)	4.00	
72	1313(8)	2332(15)	3.00	
73	1290(8)	2355(15)	2.50	
74	1279(8)	2366(15)	4.35	
75	1251(8)	2394(15)	3.70	
76	1232(6)	2413(15)	4.00	
77	1189(4)	2456(11)	6.40	
78	1161(4)	2484(11)	5.35	
79	1139(7)	2506(14)	4.20	
80	1111(4)	2534(11)	3.95	
81	1084(4)	2561(11)	5.40	
82	1070(8)	2575(15)	7.40	
83	1044(8)	2601(15)	4.20	
84	1026(8)	2619(15)	3.95	
85	1011(8)	2634(15)	4.30	
86	977(8)	2669(15)	3.55	
87	959(4)	2686(11)	12.00	
88	924(5)	2721(12)	3.95	
89	894(5)	2751(12)	3.40	
90	857(7)	2788(14)	3.40	
91	813(4)	2832(11)	10.90	
92	765(5)	2880(12)	3.15	
93	733(7)	2912(14)	3.50	
94	701(7)	2944(14)	3.25	
95	673(8)	2972(15)	7.10	
96	651(8)	2994(15)	5.40	
97	624(8)	3021(15)	...	
98	598(8)	3047(15)	...	
99	572(8)	3073(15)	10.30	
100	548(5)	3097(12)	8.50	
101	532(9)	3113(16)	7.30	
102	510(5)	3135(12)	13.60	
103	487(7)	3158(14)	6.60	
104	458(9)	3187(16)	5.75	
105	431(9)	3214(16)	6.80	
106	409(9)	3236(16)	4.85	
107	392(9)	3253(16)	4.95	
108	377(9)	3268(16)	3.30	
109	354(5)	3291(12)	6.20	
110	329(9)	3316(16)	3.90	
111	299(5)	3349(12)	9.10	
112	284(5)	3361(12)	4.20	
113	265(8)	3380(15)	5.90	
114	249(8)	3396(15)	3.95	
115	231(8)	3414(15)	3.40	
116	176(10)	3469(17)	5.95	
117	144(10)	3501(17)	4.50	
118	132(10)	3513(17)	5.40	
119	187(10)	3558(17)	5.30	
120	82(12)	3563(19)		
121	66(10)	3579(17)	5.65	
122	44(12)	3601(19)	3.65	
123	10(12)	3635(19)	4.85	
124	−31(6)	3676(13)	8.25	
125	−71(10)	3716(17)	4.90	
126	−91(10)	3736(17)	5.80	
127	−114(6)	3759(13)	6.90	
128	−164(9)	3809(16)	4.60	
129	−189(6)	3834(13)	7.20	
130	−211(6)	3856(13)	9.80	
131	−245(10)	3890(17)	3.70	
132	−265(10)	3913(17)	4.90	
133	−284	3929(17)	5.00	

the groups above group No. 40 are weighted heavily by the high-resolution 65° spectrum. The ground-state Q value was measured as 3584±12 keV for the reaction $Sm^{154}(d,p)Sm^{155}$. The observed Q values, excitation energies, and relative intensities are given in Table VI.

We have used the relative intensities observed at the

TABLE VI. Results for $Sm^{154}(d,p)Sm^{155}$. Level numbers correspond to the peak numbers in Fig. 7.

Level No.	Q (keV)	Excitation energy (keV)	Relative intensity (65°)	l value
0	3584(12)	0	1.00	0, 1, 2
1	3559(17)	25(7)	0.04	
2	3533(17)	51(7)	0.06	
3	3504(17)	80(7)	0.02	
4	3456(12)	128(2)	1.58	2, 3
5	3433(12)	151(2)	0.29	2, 3, 4
6	3357(13)	227(3)	0.12	
7	3246(13)	338(5)	0.04	
8	3219(11)	364(4)	0.17	
9	3158(10)	426(3)	0.22	
10	3085(10)	499(3)	1.14	2, 3
11	3044(12)	540(6)	0.07	
12	3022(12)	562(7)	0.06	
13	2983(12)	601(7)	0.09	
14	2967(9)	617(4)	0.17	
15	2939(12)	645(8)	0.02	
16	2868(10)	716(7)	0.05	
17	2836(10)	748(7)	0.07	
18	2798(8)	786(5)	0.18	0, 1, 2
19	2760(8)	824(5)	1.67	0, 1, 2
20	2710(8)	874(5)	0.36	
21	2675(8)	909(5)	1.99	
22	2647(8)	937(5)	1.02	
23	2621(8)	963(5)	0.89	≥ 3
24	2585(10)	999(10)	0.16	≥ 3
25	2566(10)	1018(10)	0.06	
26	2541(8)	1043(8)	0.06	
27	2508(7)	1076(7)	0.64	≥ 3
28	2477(10)	1107(10)	0.06	
29	2421(7)	1163(7)	0.11	
30	2404(11)	1180(11)	0.14	
31	2359(11)	1225(11)	0.02	
32	2245(7)	1339(7)	0.11	
33	2212(11)	1362(10)	...	
34	2176(11)	1408(10)	...	
35	2135(6)	1449(8)	0.62	
36	2097(6)	1487(8)	0.26	
37	2063(6)	1521(8)	0.29	
38	2022(10)	1561(12)	0.69	
39	2002(6)	1582(8)	1.98	
40	1995(9)	1589(11)		
41	1956(5)	1628(9)	0.67	
42	1921(6)	1663(10)	0.24	
43	1903(5)	1681(9)	0.66	
44	1868(5)	1716(9)	0.33	
45	1846(5)	1738(9)	0.49	
46	1822(5)	1762(9)	0.48	
47	1803(7)	1781(11)	0.19	
48	1783(7)	1801(11)	0.20	
49	1771(7)	1813(11)	0.25	
50	1746(5)	1838(9)	0.46	
51	1721(10)	1863(13)	0.35	
52	1696(9)	1888(12)	0.49	
53	1652(4)	1932(10)	1.44	
54	1620(6)	1964(12)	0.71	
55	1595(4)	1989(10)	0.42	
56	1574(4)	2010(10)	0.81	
57	1541(4)	2043(10)	0.51	
58	1518(4)	2066(10)	1.15	
59	1490(4)	2094(10)	1.03	
60	1471(4)	2113(10)	1.39	
61	1462(7)	2122(13)	1.80	
62	1401(4)	2180(10)	2.07	
63	1373(4)	2209(10)	0.56	
64	1339(4)	2245(10)	...	
65	1282(4)	2302(10)	1.58	
66	1240(4)	2344(10)	0.95	
67	1221(4)	2363(10)	1.23	
68	1202(4)	2382(10)	1.00	
69	1184(4)	2400(10)	2.90	
70	1153(6)	2431(12)	0.71	
71	1138(4)	2446(10)	2.17	
72	1104(4)	2480(10)	1.10	
73	1071(7)	2513(13)	1.13	
74	1037(7)	2547(13)	0.50	
75	1018(4)	2566(10)	0.30	
76	1000(4)	2584(10)	0.65	
77	985(6)	2599(12)	0.93	
78	957(8)	2627(14)	0.32	
79	914(6)	2670(12)	...	
80	865(8)	2719(14)	1.25	
81	799(4)	2785(10)	1.01	
82	755(4)	2829(10)	0.64	
83	724(4)	2860(10)	1.53	
84	697(4)	2887(10)	0.61	
85	667(4)	2917(10)	1.17	
86	639(8)	2945(14)	1.02	
87	624(4)	2960(10)	0.77	
88	564(4)	3020(10)	0.90	
89	550(8)	3034(14)	1.48	
90	509(8)	3075(14)	1.44	
91	488(8)	3096(15)	1.02	
92	457(5)	3127(11)	1.69	
93	419(8)	3165(14)	0.66	
94	383(5)	3201(11)	0.82	
95	368(9)	3216(15)	1.32	
96	323(8)	3261(14)	0.83	
97	303(5)	3281(11)	1.91	
98	284(6)	3300(12)	0.68	
99	254(5)	3330(11)	2.64	
100	234(7)	3350(13)	1.64	
101	222(7)	3362(13)	1.93	
102	184(9)	3400(15)	1.26	
103	164(9)	3420(15)	0.71	
104	134(5)	3450(11)	1.72	

various reaction angles studied in the above nuclei as a very rough guide to the approximate orbital angular momentum transfer for some of the new levels. In all cases a state which has a previously definitely determined spin and parity, or a state for which theoretical considerations allow only one possible interpretation, is available for comparison. The basic fact that allows this kind of comparison to be done is the following: The over-all change in the (d,p) cross section from forward to backward angles is a considerably larger effect than the local maxima and minima. That is, they are rather smooth functions of angle. Furthermore, the higher l values drop off considerably more slowly toward the back angles. Referring to Fig. 8, we see that $l=0$, 1, 2 could be differentiated from $l=3$, 4, 5 even on the basis of our limited data. Even such a crude distinction as this may often, when used with other knowledge, narrow the possible assignments for a level down to only one. This approach appears to work quite well in the deformed nuclei Sm^{153} and Sm^{155} where the properties of the low-lying orbitals will be very similar to the neighboring deformed nuclei.

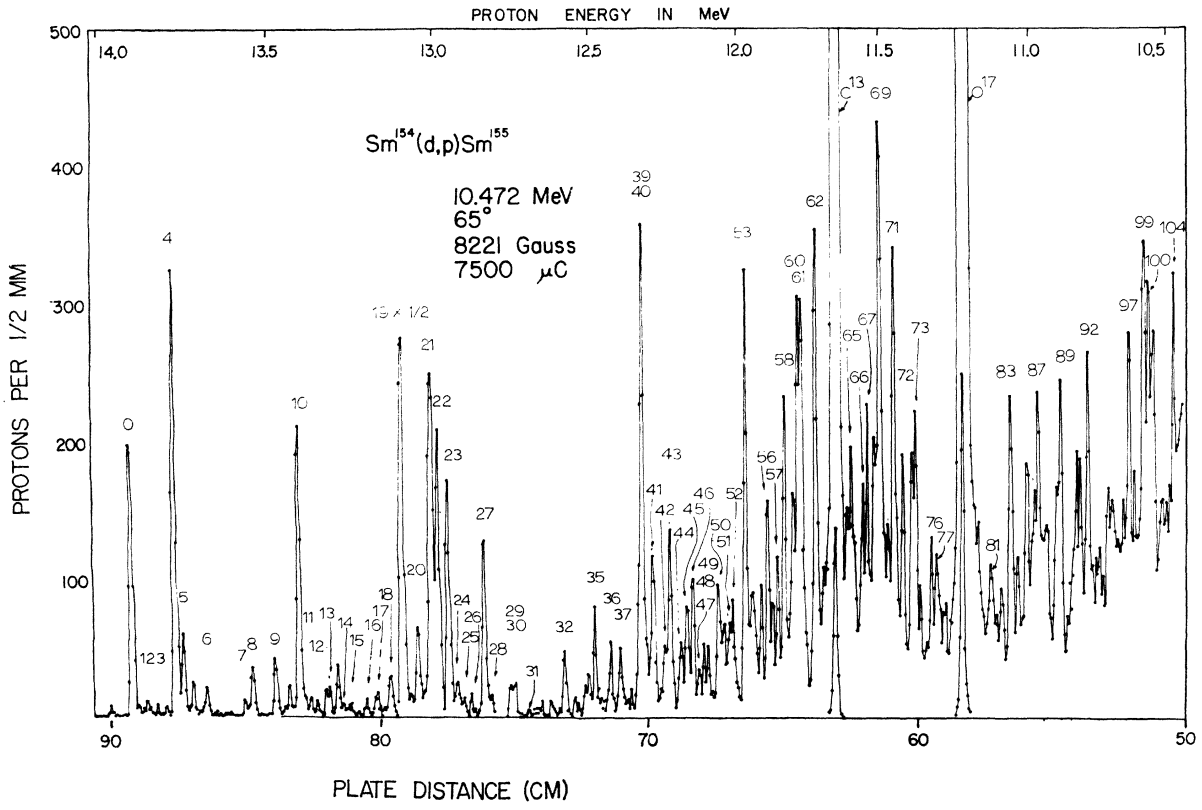

FIG. 7. The $Sm^{154}(d,p)Sm^{155}$ spectrum at 65°. Only groups assigned to Sm^{155} are numbered.

V. COMPARISON WITH PREVIOUS STUDIES

Sm^{145}

All states previously reported by Anton'eva *et al.*,[10] and Aleksandrov, *et al.*,[11] in Sm^{145} have been observed. However, our evidence for the 1004-keV level is weak and it is considered to be only tentatively verified. In addition to these levels, fifty-five new levels were determined. Owing to the relatively low (71.5%) enrichment in Sm^{144}, some of these assignments, especially the very low intensity ones, may be due to other isotopes. This is so in spite of a careful analysis designed to minimize such cases. Thirty-one groups have been rejected as due to other isotopes, but these were mainly in the higher energy part of the spectrum where the level density and background are low and accurate intensity comparisons can be made. The lower energy (higher excitation) part of the spectrum is much less definite where low-intensity groups are concerned, and the majority of erroneous assignments will be of low Q value ($Q \leq +2$ MeV).

It should be noted that the excitation energies from these (d,p) spectra are slightly higher than the β-spectrometer values (895–894, 1004–1004, 1665–1663, 1883–1880, 2002–2001, 2431–2425 keV). This trend should be kept in mind when other studies of Sm^{145} are compared with these results.

Sm^{147}

The levels in Sm^{147} at 121, 198, 800, 900, and 1420 keV deduced from the Eu^{147} decay have been confirmed by (p,p') excitation. Both the energy and the high cross section of the 708-keV level (evidently due to a large Coulomb excitation contribution) agree with the Coulomb excitation work of Nathan and Popov[15] which showed a Coulomb-excited level at ~730 keV in Sm^{147}. The level previously assigned at 1080 keV is not observed in the (p,p') spectrum. It is interesting to note that the 121 and 198-keV levels are no more intense than the higher levels, especially in the case of the 198-keV ($\frac{3}{2}^-$) level which would be Coulomb excited. This is quite different from the situation in Sm^{148}, Sm^{150}, Sm^{152}, and Sm^{154} and indicates the noncollective nature of these states.

Sm^{149}

These experiments confirm the observations of Harmatz *et al.*,[25] Schmid and Burson,[22] and Dzhelepov *et al.*,[21] on the decay of Eu^{149}. Levels at 22, 280, 350, 535, and 566 keV are observed which compare with their values of 22.5, 277.2, 350.2, 530, and 558.5 keV.

A level at 285 keV corresponds to one of the levels observed by Schmid and Burson. However, no level corresponding to the 582-keV state was observed. A

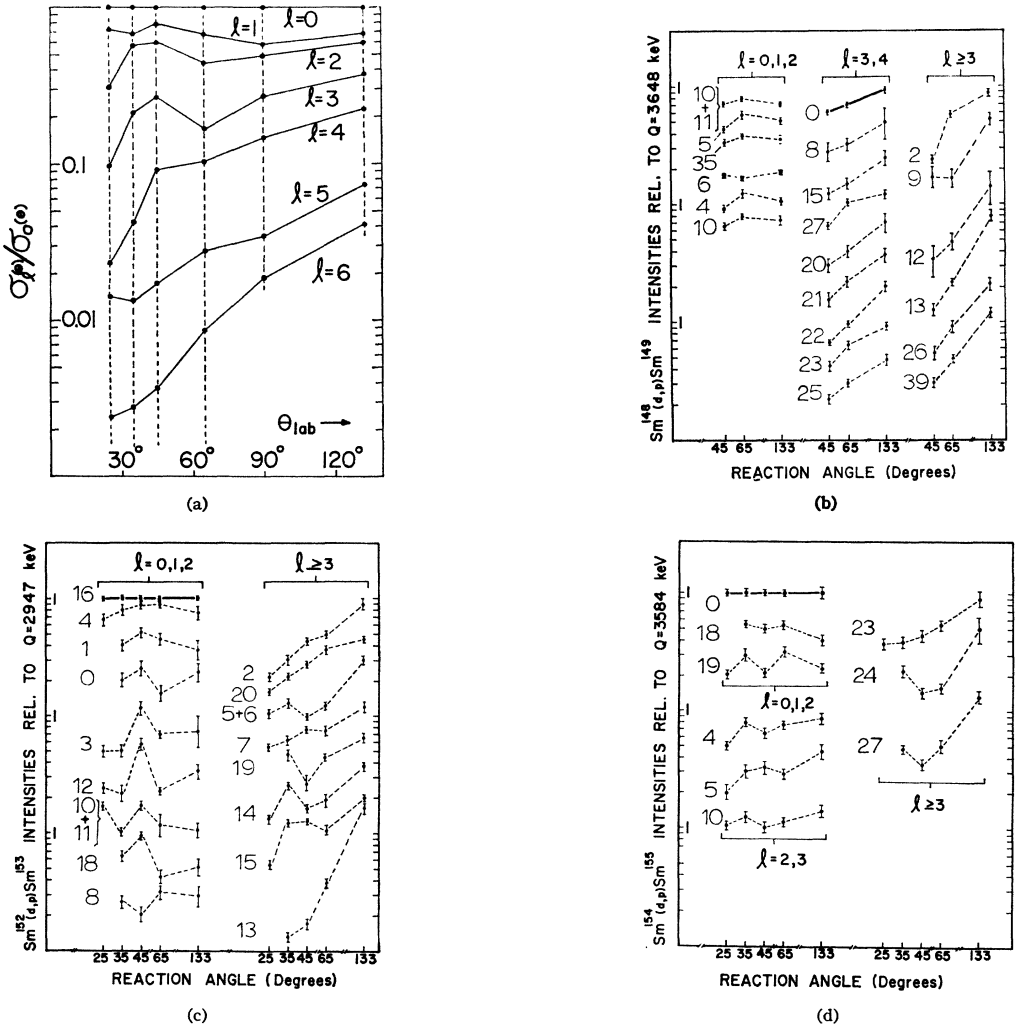

FIG. 8(a). The DWBA theoretical (d,p) intensities $\sigma_l(\phi)$ taken relative to $l=0$ for a typical rare-earth target at 12 MeV at the angles observed in these studies. (b). Observed relative intensities for $Sm^{148}(d,p)Sm^{149}$. The intensities for the reference level are connected by a solid line. For compactness of display the pattern for each level has been arbitrarily displaced vertically; however, the observed intensities at 65° (given in Table III) give directly the amount of this displacement. The identifying numbers to the left of each pattern correspond to Fig. 4 and Table III. (c). Observed relative intensities for $Sm^{152}(d,p)Sm^{153}$. The mode of display is identical to that for Fig. 8(b) and the level numbers correspond to Fig. 6 and Table V. (d). Observed relative intensities for $Sm^{154}(d,p)Sm^{155}$. The mode of display is identical to that for Fig. 8(b) and the level numbers correspond to Fig. 7 and Table VI.

weak and somewhat broad group is in evidence at 842-keV excitation, but it is too weak to definitely ascribe it to two separate levels.

Levels at 640 and 675 keV observed in these (d,p) experiments are possible candidates for the ~650-keV Coulomb-excited level which was previously observed.

Sm^{151}

By comparing the energy differences between Q values for the (d,p) peaks assigned to $Sm^{150}(d,p)Sm^{151}$ with the energy differences between Sm^{151} excited states, a correspondence may be obtained between the levels observed here and in the previous work. However, various selection rules prevent a one-to-one correspondence. The $Q=+3369$ keV and $Q=+3203$ keV ($\Delta E=166\pm5$ keV) then match the already known ground state and 168 keV levels. This then gives other points of correspondence as follows: $Q=+3158$ (209 keV), $Q=+2921$ (444 keV), $Q=+2900$ (464 keV), $Q=+2614$ (741 keV), and $Q=+2535$ (821 keV). This matching process indicates that the ground-state Q value for the reaction $Sm^{155}(d,p)Sm^{151}$ is $+3369\pm16$ keV. Excitation energies from the present study, based on the above considerations were given in Table IV.

Sm^{153}

Our data do not support the previously suggested level scheme for Sm^{153}. However, the (n,γ) data[30] on

which that scheme was based and some additional data[29] from the decay of Pm^{153} are connected with our results in the discussion of Sm^{153} in Sec. VI.

VI. DISCUSSION

Sm^{155} and Sm^{153}

Of the odd-A samarium nuclei studied here, Sm^{155} and Sm^{153} present the best opportunities for interpretation of the levels. This is due to two factors. First, the rotational $I(I+1)$ energy systematics in deformed nuclei will greatly aid in picking out such bands; second, relative strengths of (d,p) transitions in deformed odd-A nuclei can be predicted theoretically[31] in a fairly reliable way and can be used to check the levels suggested by rotational systematics. Further, working back the other way, once assignments are made we can derive information on the deformation, energy gap, moments of inertia, and single-particle level ordering by analysis of the data. The available orbitals are well known from the work of Nilsson[3] and are shown in Fig. 9 using his notation.

The energies of rotational states in an odd-A nucleus, built on a given single-particle state (in the terminology of Nilsson) are given by the relation

$$E_{JK}=E_{OK}+\frac{\hbar^2}{2\mathcal{I}}[J(J+1)-2K^2+\delta_{K\frac{1}{2}}a(-1)^{J+\frac{1}{2}}(J+\tfrac{1}{2})]$$

for a state with spin J, moment of inertia $\mathcal{I}$, and K projection on the symmetry axis Z. Rotation-vibration corrections lead to higher order terms in $I(I+1)$, but in most nuclei these have been found to be quite small. The corrections would, in most cases, go undetected for energy determinations of our precision. The decoupling parameter, a, is a unique property of bands built on $K=\frac{1}{2}$ states and can be predicted from theory.

The cross section for the (d,p) reaction on a deformed nucleus is given by

$$\frac{d\sigma}{d\Omega}=2[\sum_{\lambda}\langle l\tfrac{1}{2}\Lambda\Sigma\,|\,J\Omega\rangle a_{Nl\lambda}]^2|\,\langle u_i|u_f\rangle\,|^2U_i^2\phi_l(\theta)$$

$$=2C_J^2|\,\langle u_i|u_f\rangle\,|^2U_i^2\varphi_l(\theta)\,,$$

tum transfer to a given state is considered and we have restricted ourselves to the case of even-even targets. The $a_{Nl\lambda}$ are the expansion coefficients of the single-particle state for spherical shell-model base vectors. The C_J's are the usual vector-coupled amplitudes (tabulated in Table VII for the states considered here—see also Refs. 1 and 32), $\langle u_i|u_f\rangle$ is the vibrational overlap of the initial and final nuclei, U_i^2 is the probability that the single-particle state is empty in the target, and $\varphi_l(\theta)$ is the single-particle (d,p) stripping cross section in the direct interaction distorted-wave Born approximation (DWBA) as calculated, for example, by the codes of Tobocman,[33] Smith,[34] or Satchler.[4] The sum term can lead to remarkable variations in intensity in the states forming a band and provides valuable clues for the assignment of states; values for this term for levels of interest in Sm^{155} and Sm^{153} are shown in Table VII. U_i^2 varies in a smooth way from 0 to 1 with the level ordering over a space of about ±1 MeV.

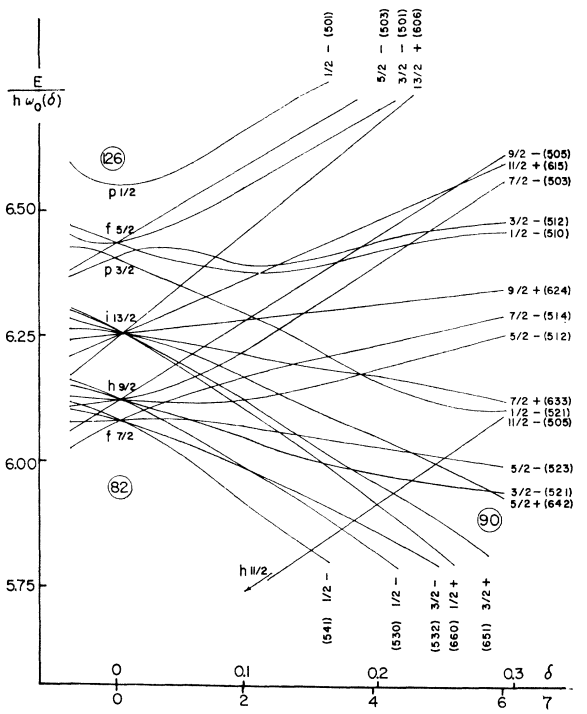

FIG. 9. The Nilsson orbitals for odd-neutron nuclei with $N=82$ to $N=126$ and $\delta\geq0$.

Although angular distributions were not taken, which could have allowed a determination of l, and absolute cross sections are not well known, which would have allowed a direct determination of C_J^2, nevertheless, relative intensities of states at the angles observed can, in some cases, provide sufficient information for assignment of certain of the single-particle bands as discussed in Sec. IV.

One can feel confident that a rotational structure will be found in Sm^{155} and Sm^{153}, since it is already well established[35] that Sm^{154} and Sm^{152} display properties of deformed nuclei. Sm^{151} is, however, in an ambiguous position since it lies between a spherical nucleus Sm^{155} and the deformed nucleus Sm^{152} (although present decay studies of Sm^{151} have been interpreted by some investi-

[31] G. R. Satchler, Ann. Phys. (N. Y.) **3**, 275 (1958).
[32] A. Isoya, Phys. Rev. **130**, 234 (1963).
[33] W. Tobocman, Phys. Rev. **115**, 98 (1959).
[34] W. R. Smith and E. V. Ivash, Phys. Rev. **128**, 1175 (1962).
[35] *Nuclear Data Sheets*, compiled by K. Way *et al.* (Printing and Publishing Office, National Academy of Science—National Research Council, Washington 25, D. C.)

TABLE VII. C_J^2 coefficients for the levels considered.

Nilsson orbital \ J		$\frac{1}{2}$	$\frac{3}{2}$	$\frac{5}{2}$	$\frac{7}{2}$	$\frac{9}{2}$	11/2	13/2
$\frac{3}{2}+$ [651] $\delta=$	0.2		~0	0.007	0.001	0.120	0.003	0.869
	0.3		~0	0.021	0.005	0.209	0.008	0.756
$\frac{3}{2}-$ [521] $\delta=$	0.2		0.067	0.003	0.551	0.323	0.058	
	0.3		0.105	~0	0.529	0.255	0.112	
$\frac{5}{2}+$ [642] $\delta=$	0.2			0.002	0.001	0.080	0.006	0.912
	0.3			0.004	0.003	0.136	0.013	0.843
$\frac{5}{2}-$ [523] $\delta=$	0.2			0.058	0.134	0.771	0.036	
	0.3			0.074	0.076	0.789	0.061	
$\frac{1}{2}-$ [521] $\delta=$	0.2	0.258	0.082	0.236	0.197	0.209	0.019	
	0.3	0.249	0.024	0.182	0.231	0.269	0.045	
(11/2)− [505] $\delta=$	0.2						1.000	
	0.3						1.000	

gators[23] in terms of rotational structure). We therefore begin the discussion of these nuclei with Sm^{155} and Sm^{153}.

Ground-State Rotational Band Assignments

For nuclei with a deformation $\delta=+0.2$ to 0.3 and $N=91$ to 93 the orbitals $\frac{3}{2}+$ (651), $\frac{5}{2}+$ (642), $\frac{3}{2}-$ (521), and $\frac{5}{2}-$ (523) are expected to be grouped closely enough to be either the ground state or located within the first 500 keV of excitation. The ground-state spin of Sm^{153} is well established experimentally[36] as $\frac{3}{2}$. The expected orbital for a deformation $\delta=0.2$ to 0.3 from the Nilsson scheme shown in Fig. 9 is the $\frac{3}{2}-$ (521) state. However, our data do not support such an assignment for the Sm^{153} ground state. This orbital would be strongly excited by the (d,p) reaction [according to the vector-addition, Nilsson coefficient sum (see Table VII) and the low l value], whereas the ground state (or, in any case, the highest observed Q value) in the $Sm^{152}(d,p)$-Sm^{153} spectra is very weak. For comparison purposes, one can examine the $Sm^{154}(d,p)Sm^{155}$ spectra (where target thickness and beam exposure is about the same), where the ground state transition is much stronger; the Sm^{155} ground state is assigned as the $\frac{3}{2}-$ (521) orbital. In making the latter ground-state assignment, we also considered the higher levels in the band; the $\frac{5}{2}-$ should be missing (and in fact is not seen) and the $\frac{7}{2}$- state should be fairly intense (as observed). At this point we can make use of the known[35] moment of inertia for this band from band structure in the neighboring nuclei Gd^{155} and Gd^{157}; this implies a $\frac{3}{2}-$ to $\frac{7}{2}-$ spacing of 130 to 145 keV. In Sm^{155} this spacing is 128 keV, which is slightly less than for Gd^{157} (these are both $N=93$ nuclei). A weak state at 227 keV in Sm^{155} is then consistent with the energy and approximate intensity of the $\frac{9}{2}-$ rotational state in this band. The lack of precision in our excitation energies does not allow a determination of small deviations from the rotational $I(I+1)$ sequence.

The excellent agreement of the $\frac{3}{2}-$ (521) band in Sm^{155} with expectations gives us confidence that the very weak ground-state group for Sm^{153} cannot be the same orbital. By comparison with Gd^{155} ($N=91$), the $\frac{3}{2}$ to $\frac{7}{2}$ energy spacing should be approximately 140 to 146 keV. The two pairs of low-lying levels which fulfill this requirement are the 34 to 177 keV and 125 to 262 keV pairs. The observation of a level at 91 keV does not favor the 34 to 177 keV combination, since (as was pointed out in Sm^{155}) the $\frac{5}{2}-$ level in the band would be expected to go unobserved. We assign the 125-keV level as $\frac{3}{2}-$ because of the high intensity of the 262-keV level (proposed as $\frac{7}{2}-$). No other low-lying state should be as strong as this one. This assignment is also consistent with the approximate l values implied by the change in relative intensities with observation angle. The ground state of Sm^{153} must then be the only other $K=\frac{3}{2}$ orbital available; namely the $\frac{3}{2}+$ (651) Nilsson orbital. Since its (d,p) strength should be negligibly weak in the Nilsson scheme, a small mixing of $\Delta N_{\hbar\omega}=\pm 2$ must be invoked to account for its observation in these experiments.

The $\frac{3}{2}-$ (521) Band

As discussed above, this orbital is located at 125 keV in Sm^{153} and is the ground state for Sm^{155}. The two γ rays from $Pm^{153} \rightarrow Sm^{153}$ of 125 keV and 180 keV[29] are then easily explained as $E1$ transitions to the ground state following an allowed β decay. We may expect that $U_i^2=0.5$. Then, since the C_J^2 term for the $\frac{7}{2}-$ rotational state has only a small dependence on deformation, we assume it has the value 0.55 for both nuclei. Using this as a calibration intensity, and getting the relative single particle intensities of the different l values from Fig. 8, a comparison of the experimental (d,p) intensities with the theoretical values can be made for the other assigned levels in the nucleus. The process may be started with the other members of the $\frac{3}{2}-$ (521) band and the results are shown in Fig. 10. The agreement is satisfactory.

The $\frac{1}{2}-$ (521) Band

According to the Nilsson scheme and the tabulated C_J^2 factors, a very strong set of states should be ob-

[36] A. Cabezas, E. Lipworth, R. Marrus, and J. Winocur, Phys. Rev. 118, 233 (1960).

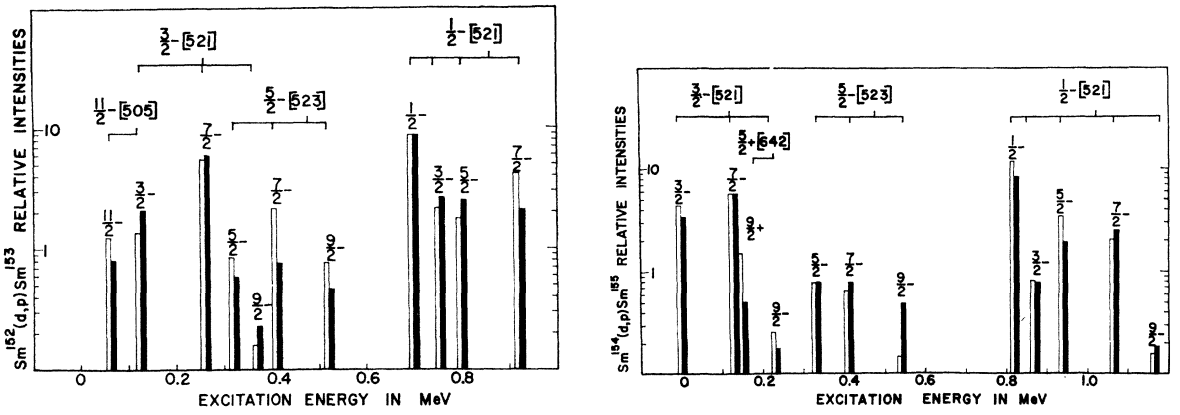

FIG. 10(a). Comparison of observed (d,p) intensities (open bars) with theory (solid bars) for $Sm^{152}(d,p)Sm^{153}$ at 45°. It was assumed that $U_i^2=0.5$ and $\delta=+0.23$. The experimental results were normalized to the theoretical intensity for the 698-keV level. (b). Comparison of observed (d,p) intensities (open bars) with theory (solid bars) for $Sm^{154}(d,p)Sm^{155}$ at 45°. It was assumed that $U_i^2=0.5$ and that $\delta=+0.30$. The experimental results were normalized to the theoretical intensity for the 128-keV level.

served somewhere between 400- and 900-keV excitation, corresponding to the $\frac{1}{2}-$ (521) band. The $\frac{1}{2}-$ member should, in fact, be the most intense single peak in the (d,p) spectrum. These bands are clearly observed to have their $\frac{1}{2}-$ band head located at 824 keV in Sm^{155} and 698 keV in Sm^{153}. The higher excitation energy for this state in Sm^{155} may be a consequence of the higher deformation depressing the ground state more than the $\frac{1}{2}-$ (521) orbital. Studies of other deformed nuclei (see for example Ref. 23) show that the relative spacing of orbitals may vary by several hundred keV from one isotope to another. The decoupling parameters for these two bands were found to be consistent with the trend previously noted in Ref. 23 for the $\frac{1}{2}-$ (521) band and we show in Fig. 11 the dependence of a and $3\hbar^2/\mathcal{I}$ on the atomic weight, including these data. The theoretical (d,p) intensities are compared with experiment in Fig. 10.

The $\frac{5}{2}-$ (523) Band

The theoretical intensities obtained from the C_J^2 factors indicate that among the low-lying bands, only the $\frac{5}{2}-$ (523) band should have appreciable intensity to its first three rotational states. The relative intensities and rotational $I(I+1)$ energy systematics should then allow its identification. Consideration of the latter properties then implies that this orbital lies at 322 keV in Sm^{153} and at 338 keV in Sm^{155}. The parameter $3\hbar^2/\mathcal{I}$ is consistent with neighboring nuclei (though slightly larger) and the relative intensities for the $J=\frac{5}{2}$, $J=\frac{7}{2}$, and $J=\frac{9}{2}$ band members are compared with theory in Fig. 10. The smaller moment of inertia probably reflects the easier deformability, because of greater neutron number, of the neighbors (Dy, Er, Yb) where this band has been previously observed.

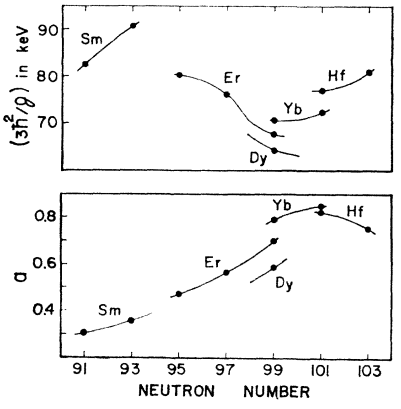

FIG. 11. Systematics of the parameters $3\hbar/\mathcal{I}$ and a for the $\frac{1}{2}-(521)$ band.

Other Bands

In Sm^{155} the only other orbital expected in the first 500 keV of excitation is the $\frac{5}{2}+$ (642) band. Although the $\frac{3}{2}+$ (651) orbital is apparently the ground state for Sm^{153}, its dependence on deformation is so large that it should be widely displaced in energy from the $\frac{3}{2}-$ (521)Sm^{155} ground state. Because of the U_i^2 dependence, this energy displacement will also decrease the intensity of the various members of the associated rotational band. Similar considerations hold in Sm^{153} for the other orbitals below the $\frac{3}{2}+$ (651). The predicted C_J^2 theoretical factors for the $\frac{5}{2}+$ (642) indicate that only the $\frac{9}{2}+$ member should show up with a measurable intensity. The approximate l value and relative intensity for the 151-keV level in Sm^{155} indicate that it is this $\frac{9}{2}+$ level. Some very weak peaks observed in one of the $Sm^{154}(d,p)Sm^{155}$ spectra may then be the $\frac{5}{2}+$ and $\frac{7}{2}+$ members of this band. The $\frac{5}{2}+$ (642) orbital would be expected to lie within 100 keV of the $\frac{3}{2}-$ (521) orbital in Sm^{155}. The moment of inertia is close to the value found for other deformed nuclei.

In Sm^{153} the $\frac{5}{2}+$ (642) band is also to be expected to lie very near the $\frac{3}{2}+$ (651) ground state. Since they are

TABLE VIII. Summary of the results of the RPC mixing effects on the $\frac{3}{2}+$ [651] and $\frac{5}{2}+$ [642] bands, for a mixing parameter $A_k=9.8$ keV.[a]

Energy[b] (keV)	$J\pi$	Original specification of intrinsic wave function	Mixing[c] amplitudes a	b	C_J	C_J^2	$(C_J^2)_{\text{exp}}$
0	$\frac{3}{2}+$	$\frac{3}{2}+$ [651]	+1.0	0	+0.031	0	0.035
36	$\frac{5}{2}+$	$\frac{3}{2}+$ [651]	+0.89	−0.455	+0.100	0.010	0.100
91	$\frac{5}{2}+$	$\frac{5}{2}+$ [642]	+0.455	+0.89	+0.125	0.015	0.035
(104)	$\frac{7}{2}+$	$\frac{3}{2}+$ [651]	+0.86	−0.51	−0.032	∼0	∼0
(162)	$\frac{7}{2}+$	$\frac{5}{2}+$ [642]	+0.51	+0.86	−0.087	0.008	∼0
176	$\frac{9}{2}+$	$\frac{3}{2}+$ [651]	+0.85	−0.52	+0.200	0.040	∼0.50
(270)	$\frac{9}{2}+$	$\frac{5}{2}+$ [642]	+0.52	+0.86	+0.551	0.300	Obsc.

[a] where $A_k=\hbar^2/2\mathcal{J}_0\,\Sigma_{lAA'}A_{lA'}(k+1)A_{lA}(k)\{\delta\varepsilon\varepsilon\,[(l-\Lambda)(l+\Lambda+1)]^{1/2}+\delta_{AA'}\}$. The indicated sum is 6.35 from the coefficients in Nilsson's paper. This implies $\hbar^2/2\mathcal{J}_0=1.54$ keV. The fact that an *exact* fit cannot be obtained for any value of A_k implies mixing from other bands unobserved here.
[b] The perturbed energies are given by $E(J)=\frac{1}{2}\{[E_k(J)+E_{k+1}(J)]\pm[(E_{k+1}(J)-E_k(J))^2+4A_k^2(J-k)(J+k+1)]^{1/2}\}$, where $A_k=|\langle k|\hbar^2/2\mathcal{J}_0 j_-|k+1\rangle|$.
[c] where $\psi_J=A\psi_{Jk}+b\psi_{Jk+1}$.

both positive parity and $K=K'+1$, a rotation-particle-coupling (RPC) effect may be expected. Kerman[37] has treated states in W^{183} in this manner and we have followed the method developed in Ref. 37 in our analysis of the mixing of the $\frac{3}{2}+$ (651) and $\frac{5}{2}+$ (642) bands in the present case. The result of this mixing leads to the following: (1) The rotational $I(I+1)$ systematics are disturbed; the $\frac{5}{2}+$, $\frac{7}{2}+$, and $\frac{9}{2}+$ members of each band are pushed apart. (2) The (d,p) strength of the $\frac{5}{2}+$ and $\frac{9}{2}+$ members of the $\frac{3}{2}+$(651) and the $\frac{5}{2}+$ (642) rotational bands is modified by the mixing. (3) Neither band had appreciable strength in the $\frac{7}{2}+$ member and this is also true for the mixed states. It seems probable that the neglected mixing effects from the $N=4$ oscillator shell account for the disagreement of the predicted (d,p) intensities for the $\frac{3}{2}+$, $\frac{5}{2}+$, and $\frac{9}{2}+$ levels with experiment. The $i_{13/2}$ shell, which is closer to the $N=4$ shell due to the spin-orbit splitting, might be expected to show such effects. The most noticeable effect due to this mixing would be on the smallest C_J coefficients.

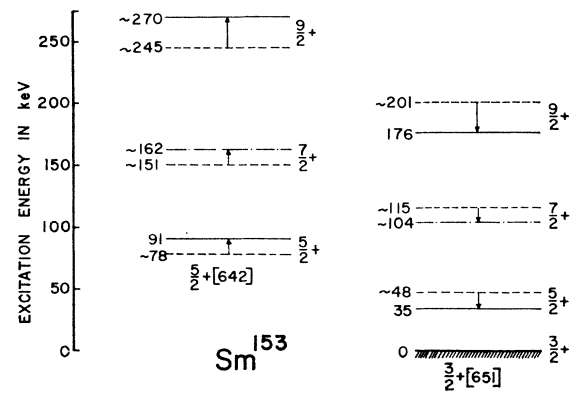

FIG. 12. Effects of rotation-particle coupling in Sm^{153}. Excitation energies are on the left and $J\pi$ assignments are on the right. Dotted lines indicate unperturbed positions, solid lines indicate observed positions, and dot-dash lines indicate postulated levels too weakly excited to be observed in this study.

[37] A. K. Kerman, Kgl. Danske Videnskab. Selskab, Mat. Fys. Medd. **30**, No. 15 (1956).

Figure 12 and Table VIII summarize the results of the (RPC) calculation for the mixing of these two bands, showing the original level positions, final positions, (d,p) intensities, and mixing coefficients.

In the above interpretation there remains a level at 65 keV in the spectrum for Sm^{153} that is unaccounted for. The observed relative intensity is very large toward backward angles compared to the neighboring levels. We suggest that its approximate l value (4 to 5) and intensity imply that it is the $11/2-$ (505) orbital. It is interesting to note that none of the γ transitions observed in the reaction $Sm^{152}(n,\gamma)Sm^{153}$ can be fitted to this level, although our interpretation of the Sm^{153} level structure accounts for most of them as $E2$, $E1$, or $M1$ transitions. Therefore, an assignment of $11/2-$ to this level is consistent with all the data. The C_J^2 factor in this case should be 1, and the observed value (based on the assumption of $C_J^2=0.25$ for the 698-keV level) is 1.5 ± 0.5. The rotational levels in the band built on the $11/2-$ (505) would not be observed since $C_J^2=0$ and $l\geq7$.

It is difficult to interpret the other states observed at higher excitation energies in these nuclei on the basis of the present information. The question of vibrational states remains open.

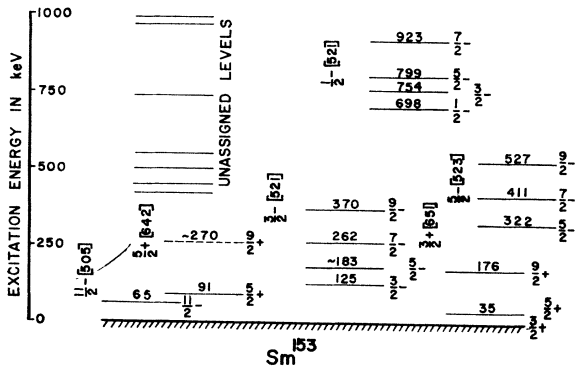

FIG. 13. A level scheme for Sm^{153} showing the assigned band structure. The dashed level at approximately 270 keV would have been hidden under the strong 262-keV level. The Nilsson assignment is given to the left of each assigned band.

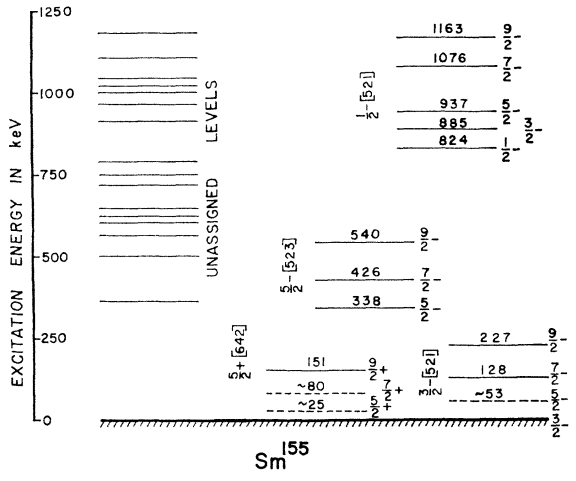

FIG. 14. A level scheme for Sm^{155} showing the assigned band structure. Dashed levels were extremely weak and only tentatively observed in one or two of the spectra. The Nilsson assignment is given to the left of each assigned band.

The band interpretations for Sm^{153} and Sm^{155} are shown in Figs. 13 and 14. The band head energies and moments of inertia given in Table IX compare well

TABLE IX. Observed moments of inertia, excitation energies and decoupling parameters.

Orbital	Nucleus	E_0 (keV)	$3\hbar^2/\mathcal{I}$ (keV)	[a]
$\frac{3}{2}+$ [651]	Sm^{153}	0	(60)[a]	...
$11/2-$ [505]	Sm^{153}	65	...	...
$\frac{3}{2}-$ [521]	Sm^{153}	125	68.5	...
	Sm^{155}	0	64.0	...
$\frac{5}{2}+$ [642]	Sm^{153}	(91)[a]	(67)[a]	...
	Sm^{155}	25	51.0	...
$\frac{5}{2}-$ [523]	Sm^{153}	322	77.0	...
	Sm^{155}	338	76.0	...
$\frac{1}{2}-$ [521]	Sm^{153}	698	82.2	+0.30
	Sm^{155}	824	90.5	+0.35

[a] These values are based on the RPC calculation of interaction between the $\frac{3}{2}+$ [651] and $\frac{5}{2}+$ [642] orbitals discussed in the text.

with those for other deformed rare-earth nuclei. It seems likely that the observed departures of the moments of inertia from those for the neighboring nuclei are due to RPC coupling which, for relatively distant bands, merely decreases $3\hbar^2/\mathcal{I}$ for the lower band and increases it for the upper band.

Sm^{151}

It seems highly probable that in this nucleus spherical and deformed nuclear shapes and their associated levels are competing for the ground state (see Sec. VII). While detailed spectroscopic assignments are possible for the neighboring nuclei Sm^{150} and Sm^{152}, this is expected to be considerably more difficult in Sm^{151} since the spectroscopy of spherical odd-A nuclei is not well understood. Perhaps the most direct method of study would be the reaction $Sm^{150}(d,p)Sm^{151}$ combined with $Sm^{152}(d,t)Sm^{151}$; it might be expected that the former would favor formation of spherical states whereas the latter would excite deformed states preferentially. [Such shape effects may have been observed recently in the reaction $Sm^{150}(t,p)Sm^{152}$]. However, (d,t) data are not yet available.

On the basis of these (d,p) data it is possible to make only a few comments on the levels in Sm^{151}. First, the previous interpretation by Harmatz, Handley, and Mihelich of a level at 168 keV as the $\frac{3}{2}-$ (521) Nilsson orbital seems to be supported by these data. We observe an intensity for this level ($Q=+3203$ keV) consistent with the assigned orbital and, in addition, observe a more intense state at 305 keV ($Q=+3062$ keV) which can be interpreted as the $\frac{7}{2}-$ rotational state in this band. The relative intensities and the moment of inertia are consistent with the other observations on this band in Sm^{153} and Sm^{155}. No definitive statement can be made about the other assignments of Ref. 23 on the basis of these data, because of the uncertainty of the coupling scheme and low intensity of the states. It appears, however, that the state we observe at ($Q=+3309$ keV) cannot be either of the two levels observed previously at 65.8 and 69.7 keV, since they should have been excited only weakly in the (d,p) reaction. It seems likely that since it is so strongly excited, this is a spherical state, and therefore might not have been observed in the previous decay work.

Sm^{147} and Sm^{149}

The ground states of Sm^{147} and Sm^{149} are known to be $\frac{7}{2}-$ and in the reaction $Sm^{148}(d,p)Sm^{149}$ this state is strongly excited. This would be expected in a shell-model interpretation. Although Sm^{146} is not available as a target, (d,p) on Sm^{144} shows a strong (d,p) cross section to the $\frac{7}{2}-$ ground state of Sm^{145} and we can be reasonably certain that the three nuclei Sm^{145}, Sm^{147}, and Sm^{149} have ground states well described by the shell-model and seniority coupling.

In $Sm^{147}(p,p')Sm^{147}$ it is possible to exploit to some extent the predominantly direct nature of the interaction [known to be mostly direct from (p,p') experiments[6,38] on other samarium nuclei], by describing the excited states as coupling of an $f_{7/2}$ neutron to the 2+ vibrational state of Sm^{146}. This approach has had success in other nuclei.[39] The 2+ state of Sm^{146} lies at 748 keV and by coupling $f_{7/2}$ to it we can obtain five states: $\frac{3}{2}-$, $\frac{5}{2}-$, $\frac{7}{2}-$, $\frac{9}{2}-$, and $11/2-$. The center of gravity of these states, defined as

$$\sum_J E_J(2J+1)/(2J_0+1)(2J_{\text{core}}+1),$$

should be at about 750 keV, they should all be characterized by $l=2$ distributions, and their relative cross

[38] R. A. Kenefick and R. K. Sheline, Phys. Rev. 135, B939 (1964).

[39] F. Perey, R. J. Silva, and G. R. Satchler, Phys. Letters 4, 25 (1963).

TABLE X. Relative intensitites for $Sm^{147}(p,p')Sm^{147}$ compared with the surface phonon and the $f_{7/2}^3$ models.

Level no.	Energy (keV)	122½° I_{exp}	122½° $I_{f_{7/2}^3}$	133° I_{exp}	133° $I_{f_{7/2}^3}$	I_{phonon}
1	121	4.5	4.5[a]	2.95	2.95[a]	3
2	198	2.0[a]	2.0[a]	2.0[a]	2.0[a]	2[a]
3	708	Obsc.		4.5	5.65 ($J=11/2$)	4 ($J=\frac{7}{2}$) 5 ($J=\frac{9}{2}$) 6 ($J=11/2$)
4	802	0.5		Obsc.		
5	919	1.1		0.9		
6	1020	Obsc.		1.45		
7	1053	2.2		1.5		
8	1097	3.8	3.16 ($J=\frac{9}{2}$)	4.3	2.86 ($J=\frac{9}{2}$)	4 ($J=\frac{7}{2}$)
9	1162	0.90		0.7		
10	1214	0.20		0.16		
11	1310	2.2		Obsc.		

[a] The intensity of the 198-keV level was set arbitrarily at 2.0. The predicted intensity of the $(f_{7/2})^3$ model was fitted to levels 1 and 2 in order to fix σ_4/σ_2 and σ_6/σ_2.

sections should be proportional to $(2J+1)$. We compare in Table X the relative intensities of the levels in $Sm^{147}(p,p')Sm^{147}$ with these predictions.

An alternative approach is that used by Funsten *et al.*,[5] in analyzing the reaction $V^{51}(p,p')V^{51}$ at 19 MeV [V^{51} is also an $(f_{7/2})^3$ configuration]. Then in DWBA the inelastic cross sections are given by

$$\frac{d\sigma}{d\Omega}=\frac{2J_f+1}{2J_i+1}V_g^2\sum_l\frac{M_l^2}{2l+1}\sigma_l(\theta),$$

where J_f and J_i are the final and initial spins, V_g is a two-body interaction depth, and M_l^2 is the integrated angular part of the interaction matrix element, summed over the allowed l's. Since we do not have angular distributions it is only possible to interpret the character of states up to a necessary, but not sufficient, specification. However, some tentative interpretations can be made on this basis. The M_l's are given in Ref. 5 for the excited states $\frac{3}{2}$, $\frac{5}{2}$, $\frac{9}{2}$, 11/2, and 15/2. Assuming that such a description is valid, it is possible to obtain the ratio σ_4/σ_2 from the known $\frac{5}{2}-$ and $\frac{3}{2}-$ states at 121 and 198 keV in Sm^{147} since the contribution from $l=6$ in the former cross section is so small. After obtaining the σ_4/σ_2 ratio from the observed cross sections for the first two excited states, the relative intensities for the other $\nu=3$ states are calculable. The relative cross sections are given by

$$\sigma_{3/2}=4[(0.065)(\sigma_2/5)+(0.117)(\sigma_4/9)],$$
$$\sigma_{5/2}=6[(0.185)(\sigma_2/5)+(0.009)(\sigma_4/9)+(0.024)(\sigma_6/13)],$$
$$\sigma_{9/2}=10[(0.031)(\sigma_2/5)+(0.097)(\sigma_4/9)+(0.0184)(\sigma_6/13)],$$
$$\sigma_{11/2}=12[(0.084)(\sigma_2/5)+(0.0293)(\sigma_4/9)+(0.039)(\sigma_6/13)],$$
$$\sigma_{15/2}=16[(0.034)(\sigma_4/9)+(0.0573)(\sigma_6/13)].$$

Neglecting the σ_6 term in the $\sigma_{5/2}$ cross section, we obtain $\sigma_4/\sigma_2=0.45$ (at 122°) and $\sigma_4/\sigma_2=0.9$ (at 133°). The σ_6 term is important only for the 15/2− state, and we obtain upper and lower limits for $\sigma_{15/2}$ by letting $\sigma_6/\sigma_4=1$ and 0, respectively. The results are compared with the data in Table X. The agreement of theory with experiment is not particularly good for either the $(f_{7/2})^3$ or the phonon approach. However, it does appear from these data that the level at 708 keV has a $J\pi$ value of $\frac{7}{2}-$ to 11/2− and the 1097-keV level has a $J\pi$ value of $\frac{7}{2}-$ or $\frac{9}{2}-$. It is interesting to note that both these levels were unobservable in the studies of the decay of Eu^{147}, although other high spin levels were populated. A recent pairing-model calculation[40] predicts a $\frac{7}{2}-$ level at 622 keV, which is reasonably close to the most intense inelastic level (708 keV). The octupole state is known[41] to lie at 1165 keV in Sm^{148}, and coupling to this core state would produce a large number of additional states which would be excited in (p,p') reactions. Therefore, it is impossible to make any comments concerning the other observed levels.

We may approach the levels of Sm^{149} on the basis of the $(f_{7/2})^{-3}$ configuration. Then the possible states should be similar to those for Sm^{147}, except for the effects of the residual interactions. If we take the Sm^{148} nucleus as a pure $(f_{7/2})^4$ configuration with seniority $\nu=0$ then the stripping amplitudes to the various states may be calculated. Clearly, since $\nu=0$, in the target, only the $\nu=1$, $J\pi=\frac{7}{2}-$ state in Sm^{149} nucleus can be excited. The ground state is known to be $\frac{7}{2}-$ and is very intense in the (d,p) spectrum. Therefore, we have taken its relative intensity as a representative $l=3$ transition in Fig. 8(b). The observed trend of relative intensity for the doublet at 277–285 keV indicates an l definitely greater than 3 and is thus quite consistent with previous assignments of $\frac{9}{2}-$ for these states. However, the data do not support a high l-value assignment to the 350-keV level. An $l<3$ is indicated for this level. A large number

[40] F. J. Schima, Doctoral thesis, University of Notre Dame, 1963 (unpublished).
[41] O. Hansen and O. Nathan, Nucl. Phys. 42, 197 (1963).

of levels of apparent high and low l value were observed for this nucleus [see Fig. 8(b)], but their interpretation will await more definite evidence than is presently available.

Sm^{145}

Since the (d,p) reaction corresponds to dropping a neutron into the target configuration, which here is closed in neutrons at $N=82$, we should be seeing the single-particle neutron states expected in the shell model. Considerable previous work has been done[42,43] on the neighboring $N=82$ nuclei (Ba^{138}, Ce^{140}, and Nd^{142}) for the (d,p) reaction and has established energy splitting which can be used to discuss our results for $Sm^{144}(d,p)Sm^{145}$.

From the previous (d,p) work and the decay work it is clear that the ground state and 894-keV states so strongly excited in $Sm^{144}(d,p)Sm^{145}$ are the $f_{7/2}$ and $p_{3/2}$ single-neutron states. Our observed spacing compares with 650 keV for Ba^{139}, 670 keV for Ce^{141}, and 718 keV in Nd^{143}. The (d,p) excited state at 1108 keV seems to correspond to the second $\frac{3}{2}-$ (presumably $p_{3/2}$) state which is found at 1100 keV in Ba^{139} and the doublet 1090–1140 keV in Ce^{141}. The observed energy spacings and relative intensities are reasonable and consistent with these assignments. The 1003-keV state, which is very weakly excited in the (d,p) spectra, is found to decay by $M1$ radiation to the $\frac{3}{2}-$ 894-keV state,[11] which means it is $\frac{1}{2}-$, $\frac{3}{2}-$, or $\frac{5}{2}-$ in nature. The only analogous weakly excited state in the other two nuclei is the proposed $\frac{5}{2}$ level at 1500 keV in Ce^{141}. Angular distributions would be necessary to confirm this hypothesis. The other very strong states in the (d,p) spectrum occur at 1611, 1665, 1971, and 2002 keV. The second and fourth of these are also (within the estimated energy error) observed in the decay of Eu^{145} and from the decay are limited to $\frac{3}{2}$, $\frac{5}{2}$, $\frac{7}{2}$, and $\frac{3}{2}$ to $\frac{9}{2}$ spins, respectively. As such they can arise only from the $f_{5/2}$ or $g_{9/2}$ single-neutron shell, model orbitals. A more exact assignment cannot be made on the basis of the present information.

VII. CONCLUSIONS

One of the results from this study of level systematics in the Sm isotopes is evidence indicating that spherical and deformed nuclear shapes may exist close to the ground state in Sm^{151}. Although it is normally assumed that states in a given nucleus have a common character and common shape, Mottelson and Nilsson[44] have suggested that quite different prolate deformations may occur within the same nucleus, particularly in the region of 90 neutrons. The forbiddenness of the 50±16 keV

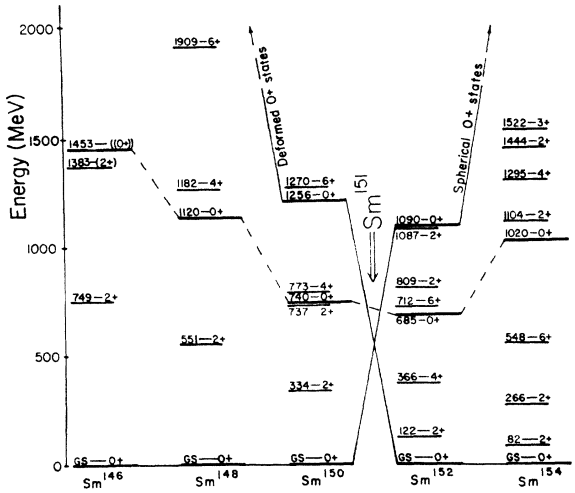

FIG. 15. Levels of even-even Sm isotopes. Bold-faced lines emphasize $Q+$ states. The sets of spherical and deformed $0+$ states are connected by solid lines. Spherical and deformed vibrational $0+$ states are connected by dashed lines. The data are taken from Refs. 38, 46, and 6.

$M3$ transition of the 9.3 hour isomer of Eu^{152} has been interpreted in these terms. In O^{16} there is evidence[45] of the existence of spherical, prolate, and oblate shapes at 0, 6.06, and 11.25 MeV, respectively. It is therefore not unreasonable to look for different shapes and their associated spectra in the same nucleus here in this transition region. There exist two sets of evidence for the presence of both deformations in Sm^{151} at low excitation.

(1). Figure 15 presents the levels for even-even Sm nuclei. Data are mostly obtained from Refs. 6, 35, and 38. However, the level observed at 1090 keV in the very important recent experimental work of Hinds *et al.*,[46] is not only an important new $0+$ state, but the cross section observed in the (t,p) reaction is strong evidence for a spherical character. A state at approximately 1100 keV in Sm^{150} is inferred from the calculations of Bes and Szymanski.[47] We associate the previously observed[20,48,49] $0+$ level at 1256 keV with this theoretically predicted state because the previous study of the reactions $Sm^{149}(d,p)Sm^{150}$ and $Sm^{150}(p,p')Sm^{150}$ showed no trace of excitation of this level. Excitation of such a deformed state from these spherical targets is expected to be strongly inhibited because of the large change in shape. Solid lines have been drawn in Fig. 15 connecting the spherical ground states up to Sm^{150}, and then up to the 1090-keV state in Sm^{152}. Conversely, the solid line connecting the prolate deformed states sweep down from Sm^{150} and become the ground states in Sm^{152},

[42] R. H. Fulmer, A. L. McCarthy, and B. L. Cohen, Phys. Rev. **128**, 1302 (1962).
[43] F. W. Bingham and M. B. Sampson, Phys. Rev. **128**, 1796 (1962).
[44] B. R. Mottelson and S. G. Nilsson, Kgl. Danske Videnskab. Selskab, Mat. Fys. Skrifter **1**, No. 8 (1959).
[45] J. Borysowicz and R. K. Sheline, Phys. Letters **12**, 219 (1964).
[46] S. Hinds, J. H. Bjerregaard, O. Hansen, and O. Nathan, Phys. Letters **14**, 48 (1965).
[47] D. R. Bes and Z. Szymanski, Nucl. Phys. **28**, 42 (1961).
[48] R. A. Ricci, R. Van Lieshout, G. B. Vingiani, S. Momaro, and B. Van Nooijen, Nucl. Phys. **32**, 490 (1962).
[49] L. V. Groshev, A. M. Demidov, V. A. Ivanov, V. N. Lutsenko, and V. I. Pelekhov, Nucl. Phys. **43**, 669 (1963).

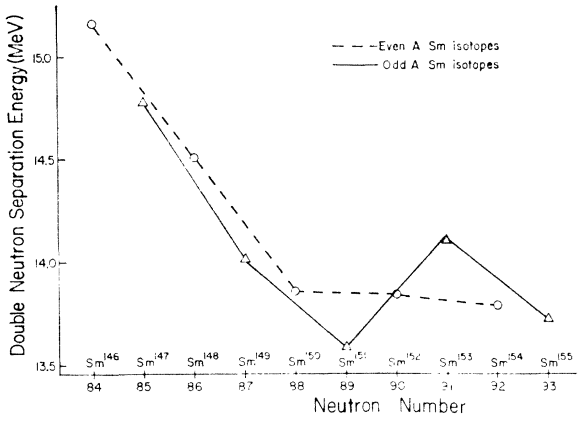

FIG. 16. Double-neutron separation energies (S_{2n}) for even-even (dashed line) and odd-A (solid line) Sm isotopes plotted against neutron number. Data are taken from Refs. 6, 38, and 50, as well as this paper. There is approximate agreement between the (d,p) Q values of Refs. 6, 38, and this paper and those of Ref. 50. The S_{2n} from Ref. 50 are 78 and 44 keV lower for Sm^{149} and Sm^{150}, respectively, than those obtained here. Although these differences are greater than either set of probable errors, they do not in any way effect the conclusions drawn here.

Sm^{154}, etc. Thus we see that the transition from Sm^{150} to Sm^{152} is quite abrupt. The 89-neutron nucleus Sm^{151}, where the deformed and spherical lines cross in Fig. 15, might then be expected to display both spherical and deformed shapes and associated spectra close to the ground state.

(2). Discontinuities in the two-neutron separation energies (S_{2n}) are plotted in Fig. 16. These discontinuities are evidence for a change in the shape and character of ground states. Barber *et al.*,[50] have recently published S_{2n} for the even-A Sm isotopes. These data together with the S_{2n} for odd-A Sm isotopes are plotted in Fig. 16. In addition to the fact that the discontinuity is more abrupt in the odd-A than in the previously studied even-even Sm isotopes, it occurs between Sm^{151} and Sm^{153} rather than between Sm^{149} and Sm^{151}. The relative continuity between S_{2n} of Sm^{151} and the lighter sperical odd-A Sm isotopes suggests that either the ground state of Sm^{151} is spherical or that a spherical state lies close to the ground state in this nucleus. It is also interesting to note that the trend in 2-neutron separation energies is reversed before and after the onset of deformation. This effect may be due in part to the fact that odd-A nuclei have a greater deformation than their even-even neighbors. The data for these two-neutron separation energies are presented in Table XI.

Of course, the most convincing evidence would be the complete identification and spectroscopic assignment of each state in Sm^{151}—some to a spherical shape and others to a deformed shape. The possibility of performing (d,p) and (d,t) reactions from a spherical and deformed target, respectively, leading to the common 89-neutron species, has been previously suggested in this paper. Such a possibility exists for study of Nd^{149}, Sm^{151}, Eu^{152}, and Gd^{153}. Experiments on Nd^{149} and Eu^{152} are now being performed at Florida State University. It seems that levels associated with spherical, prolate, and oblate shapes can all exist in a given nucleus. The energetic threshold for the appearance of these shapes will vary from nucleus to nucleus, making a set of energy surfaces as a function of neutron and proton number. These energy surfaces for the spherical and prolate deformed shapes appear from the above discussion to intersect very close to the ground state in Sm^{151}, and this would hold true for other 89-neutron species. The implications in terms of greater richness of spectroscopic detail and for such phenomena as the nuclear Franck-Condon principle are indeed intriguing.

TABLE XI. Two-neutron separation energies for the Sm isotopes. Data are taken from Refs. 6, 38, and 50, and also from this work.

Nucleus	Two-neutron separation energy (S_{2n}) (in MeV)
Sm^{146}	15.168±0.032
Sm^{147}	14.782±0.035
Sm^{148}	14.517±0.030
Sm^{149}	14.018±0.015
Sm^{150}	13.862±0.013
Sm^{151}	13.583±0.017
Sm^{152}	13.842±0.005
Sm^{153}	14.118±0.013
Sm^{154}	13.794±0.005
Sm^{155}	13.728±0.013

This study of the odd-A Sm isotopes has also yielded detailed spectroscopic assignments, particularly for Sm^{153} and Sm^{155}. A summary of this spectroscopic information is as follows:

(1) These data for Sm^{145} are in substantial agreement with the previous studies of other $N=83$ nuclei based on a single-particle interpretation.

(2). A qualitative interpretation of the levels in Sm^{147} is possible using either an excited core coupled to an $f_{7/2}$ neutron or by using the $(f_{7/2})^3$ configuration. However, these data are too sketchy to do more than suggest a few high-spin possibilities based on either of these configurations. In any case, the number of low-lying levels is far in excess of these simple predictions.

(3). Detailed spectroscopic assignments for Sm^{151} are difficult as described above. However, the existence of both spherical and deformed shapes low in the excitation spectrum seems to be indicated.

(4). Detailed spectroscopic assignments in Sm^{153} and Sm^{155} have been made. The characteristic (d,p) intensities of members of rotational bands, together with energies of these levels, and the systematics of other deformed odd-A nuclei, have made possible these assignments. Definite evidence was found for the assignment of the $\frac{3}{2}-$ (521), $\frac{5}{2}-$ (523), and $\frac{1}{2}-$ (521) orbitals

[50] R. C. Barber, H. E. Duckworth, B. G. Hogg, J. D. Macdougall, W. McLatchie, and P. Van Rookhuyzen, Phys. Rev. Letters **12**, 505 (1964).

in Sm^{153} and Sm^{155}. Systematics of the moments of inertia and the decoupling parameter, where applicable, have been studied. A surprising increase in the parameter $3\hbar^2/\mathcal{I}$ for the $\frac{1}{2}-$ (521) band has been found in going from Sm^{153} to Sm^{155}. Of particular interest is the tentative assignment of the previously unidentified $11/2-$ (505) state in Sm^{153}. The depopulation of this state is hypothesized to account for the sudden onset of deformation at $N=90$. Identification of the expected positive-parity states in Sm^{153} and Sm^{155} has proved difficult. The primary cause of the difficulty is to be found in the very small amplitudes for the low-l-value spherical-oscillator base vectors in the deformed intrinsic wave functions, in the case of positive parity. This caused considerable difficulty in the interpretation of Sm^{153} where the positive-parity states are of crucial importance. Although the level scheme proposed here for Sm^{153} is not completely satisfactory concerning the (d,p) intensities to the low-lying $\frac{3}{2}+$ (651) and $\frac{5}{2}+$ (642) states (see Sec. VI), it is fairly consistent with the available (n,γ) and Pm^{153} decay data and also with the expected locations of the Nilsson orbitals for $N=91$. A large number of alternative level schemes for Sm^{153}, involving for example the $\frac{1}{2}+$ (660) or $\frac{3}{2}-$ (532) orbitals and the possibility that the ground state was not observed by (d,p), were carefully considered and rejected as not consistent with all the known data. A calculation of the magnetic moment for the assigned $\frac{3}{2}+$ (651) orbital in the strong-coupling limit gives $\mu=-0.36$ ($\delta=+0.3$) and $\mu=-0.24$ ($\delta=+0.2$) nuclear magnetons using Nilsson's base vectors. These are closer to the experimental value[35] of -0.055 that the calculated values of -0.54 ($\delta=+0.3$) and -0.31 ($\delta=+0.2$) for the $\frac{3}{2}-$ (521) orbital. The discrepancy between theory and experiment perhaps indicates an inaccuracy in Nilsson's $A_{nl\Lambda}$ coefficients; this could also account for the observed discrepancies in the (d,p) intensities to the positive-parity states. Assignment of the Sm^{153} ground state as the $\frac{3}{2}+$ (651) orbital does not necessarily change the shape arguments used to explain[44] the decay of Sm^{153} to Eu^{153} although the most intense β transitions become a-h (allowed-but-hindered) in character. This is not inconsistent with the log ft values. In particular, a-h character is much more consistent with the log $ft=7.3$ ground-state β branch than the $1h$ previous characterization (there are no other known $1h$ transitions with log $ft<8$). The observation of the $\frac{3}{2}+$ (651) ground state, the poor agreement of the (d,p) intensities to the $\frac{3}{2}+$ (651) and $\frac{5}{2}+$ (642) RPC-interacting bands with the predictions of the Nilsson coefficients, and the unreasonably small value of $\hbar^2/2\mathcal{I}_0$ implied by the A_k parameter using the Nilsson coefficients may indicate that these coefficients are not accurate in the case of the $i_{13/2}$ orbits. Available evidence[23] on the RPC interaction between the $\frac{3}{2}+$ (651) and $\frac{5}{2}+$ (642) bands in Gd^{155} also supports this possibility. It is tentatively suggested that the unusually large splitting of the $i_{13/2}$ and $i_{11/2}$ orbitals is responsible. The $i_{13/2}$ orbital is depressed until it is approximately equally distant from the $N=4$ states and the other $N=6$ states. This requires inclusion of the $N=4$ states in calculations of the $A_{nl\Lambda}$ amplitudes. Furthermore, since some of the $N=4$ contributions to the $A_{nl\Lambda}$ would be of opposite sign, the factor $\langle k|J_-|k+1\rangle$ would be reduced and then might imply a physically reasonable $\hbar^2/2\mathcal{I}_0$ for the RPC interaction. There is, of course, the possibility of inaccurate $N=6$ coefficients caused by imperfect values for C and D in the Hamiltonian terms $C(\mathbf{l}\,\mathbf{s})$ and $D(\mathbf{l}\,\mathbf{l})$.

It is felt that the question of spherical versus deformed states in $N=89$ nuclei and more far-reaching calculations of the nature of orbitals arising from the $i_{13/2}$ multiplet are topics worthy of further investigation.

ACKNOWLEDGMENTS

We are grateful to R. Harlan, C. Nealy, R. Jernigan, and H. Kaufmann, for aid in data-taking and reduction, to E. Wehunt, S. Hipps, and M. Jones for plate reading, and to K. T. Hecht for helpful conversations.